

Gravitational Bremsstrahlung in Black-Hole Scattering at $\mathcal{O}(G^3)$: Quadratic-in-Spin Effects

Lara Bohnenblust,¹ Harald Ita,^{1,2} Manfred Kraus,³ Johannes Schlenk¹

¹*Department of Astrophysics, University of Zurich, Winterthurerstrasse 190, 8057 Zurich, Switzerland*

²*Paul Scherrer Institut, CH-5232 Villigen PSI, Switzerland*

³*Departamento de Física Teórica, Instituto de Física, Universidad Nacional Autónoma de México, Cd. de México C.P. 04510, México*

E-mail: lara.bohnenblust@uzh.ch, harald.ita@psi.ch,
mkraus@fisica.unam.mx, johannes.schlenk@psi.ch

ABSTRACT: We are employing a supersymmetric variant of the worldline quantum field theory (WQFT) formalism to compute the far-field momentum-space gravitational waveform emitted during the scattering of two spinning black holes at next-to-leading order (NLO) in the post-Minkowskian expansion. Our results are accurate up to quadratic-in-spin contributions, which means we report for the very first time the waveform observable at the order $\mathcal{O}(G^3\mathcal{S}^2)$. Our computation is based on mapping n -body tree-level amplitudes in such a way that we can obtain the $(n-2)$ -loop two-body waveform integrand. We discuss in detail this procedure and highlight the similarity of the resulting structures with those obtained in the scattering-amplitude approach. As a by product of our computational approach, we also obtain, for the first time, the leading-order waveform for three-body scattering of spinning black holes. We validated our results in various ways but most notably, we find exact agreement for the NLO waveform integrand obtained from the WQFT and the classical limit of scattering amplitudes in QFT.

Contents

| | | |
|----------|--|-----------|
| 1 | Introduction | 2 |
| 2 | Setup, notation and kinematics | 3 |
| 3 | Waveforms from the worldline QFT formalism | 5 |
| 3.1 | The worldline theory and weak-field expansion | 6 |
| 3.2 | The gravitational waveform | 7 |
| 3.3 | Classical metric from worldline QFT | 8 |
| 3.4 | Feynman rules | 9 |
| 3.5 | Classical amplitudes | 11 |
| 3.6 | Two-body scattering from seven-point trees | 15 |
| 4 | Waveform computation | 19 |
| 4.1 | Amplitude computation | 19 |
| 4.2 | Integrals | 21 |
| 5 | Spinning waveforms from QFT amplitudes | 23 |
| 6 | Results | 27 |
| 6.1 | Leading-order three-body momentum-space waveform | 27 |
| 6.2 | Next-to-leading order two-body momentum-space waveform | 27 |
| 6.3 | BMS frame | 30 |
| 6.4 | Validation | 30 |
| 7 | Conclusion | 31 |
| A | Feynman rules | 32 |
| B | Worldline supersymmetry property | 34 |

1 Introduction

Since the first detection of gravitational waves [1–5] by LIGO and Virgo, the study of gravitational radiation from compact binary systems has advanced significantly. Detector sensitivities have steadily improved, and to date, the LIGO-Virgo-KAGRA (LVK) collaboration has reported 90 merger events involving compact objects [6]. Looking ahead, next-generation observatories such as the Einstein Telescope, Cosmic Explorer, TianQin, and the Laser Interferometer Space Antenna (LISA) promise to probe gravitational waves with even greater sensitivity and across a broader frequency range [7–10]. These advances will enable deeper exploration of binary parameters, including spin and orbital eccentricity.

A central theoretical challenge in this context is the accurate and efficient modeling of gravitational waveforms from such systems [11, 12]. Black holes and neutron stars are often highly spinning, and their spins significantly affect the dynamics of the inspiral [13–19]. This is particularly true when the spin vectors are misaligned with the orbital angular momentum, leading to orbital precession and phase modulations in the gravitational waveform. Capturing these spin effects is essential for building high-precision waveform models that can fully exploit the scientific potential of current and future gravitational wave observations.

To meet this precision challenge, several analytical frameworks have been developed. Both the post-Newtonian (PN) and, more recently, the post-Minkowskian (PM) expansions have seen tremendous progress in the analytical study of two-body dynamics. In the PN framework, results have been obtained through classical methods [17, 20–38] as well as effective field theory (EFT) approaches [39–72]. On the other hand, the PM expansion is more naturally employed in quantum field theoretical methods based either on scattering amplitudes [73–119] or the worldline quantum field theory (WQFT) [120–123] to describe the *scattering* of black holes. A different and orthogonal approach is the self-force expansion [124–136] in which one computes to all orders in the Newton constant G_N but expands in the mass-ratio of the black holes.

Here, we focus on the PM approach and extend previous results for black-hole scattering waveforms. The leading-order (LO) result for non-spinning black holes has long been known from classical general relativity [137–139]. These results were rederived in the WQFT [140, 141] and the up to all-order-in-spin corrections were added in refs. [142–145]. Since then, next-to-leading order (NLO) results at $\mathcal{O}(G^3)$ were obtained from scattering amplitudes in a QFT [146–150], using the Kosower-Maybee-O’Connell (KMOC) formalism [151–153]. In ref. [154], consistency between the MPM framework and amplitude-based results was established. The linear-in-spin correction to the NLO waveform at $\mathcal{O}(G^3\mathcal{S})$ was subsequently computed [150] using amplitude methods and cross-checked against a WQFT calculation.

In this paper, we extend the PM NLO scattering waveform by including quadratic-in-spin corrections at $\mathcal{O}(G^3\mathcal{S}^2)$. To systematically organize the classical perturbation theory, we employ both WQFT and standard QFT methods. In particular, we focus on the diagrammatic structure of the WQFT to make the mass dependence and classical spin contributions manifest. The one-loop WQFT integrand is constructed from seven-point

tree-level amplitudes, which serve as generating building blocks (see e.g. [120, 155]). In contrast to the WQFT, the amplitude-based approach offers well-known and well-tested Feynman rules, which we use to cross-check our results. For validation, we make use of a numerical implementation [150, 156] of the relevant amplitudes. This comparison also includes an implementation of the Casimir \mathcal{S}^2 contributions, which is based on the *spin-interpolation* method of refs. [113, 117] and confirms its validity. The spectral waveform requires momentum integration associated to the exchanged radiation, which resembles the one of one-loop Feynman integrals. The retarded momentum integrals are shown to match the known integral basis [157] obtained within the KMOC formalism.

This article is organized as follows: In section 2 we state our conventions and introduce our choice of kinematical variables. In section 3 we briefly summarize the WQFT formalism and lay out our strategy to compute the gravitational waveform at NLO. Then, in section 4 we give further details on the explicit computation. In section 5 we discuss how to perform the corresponding calculation in a scattering-amplitude setup. In section 6 we present our results and in section 7 we summarize our conclusions.

2 Setup, notation and kinematics

We consider the scattering of two compact spinning objects, described as point masses (m_i) and with spin \mathcal{S}_i . We assume the objects Compton wavelength $\lambda_c \sim 1/m_i$ to be much smaller than their Schwarzschild radius $r_{s,i} = 2Gm_i$, such that $Gm_i^2 \gg 1$. The scattering is assumed to take place with an impact parameter $b = |b_1 - b_2|$ much larger than the objects' Schwarzschild radius, which implies the classical weak-field regime with $b \gg r_{s,i}$. The spin is assumed to be classical and small enough, such that the ring radius $a_i = \mathcal{S}_i/m_i$ is much smaller than the Schwarzschild radius $a_i/r_{s,i} \ll 1$, and we treat it perturbatively. The system emits gravitational radiation and we compute its waveform at large distance $|r| \gg b$ from the scattering objects at $\mathcal{O}(G^3\mathcal{S}^2)$. A pictogram of the considered process with relevant quantities indicated is shown in fig. 1. Below we will mostly refer to the scattering

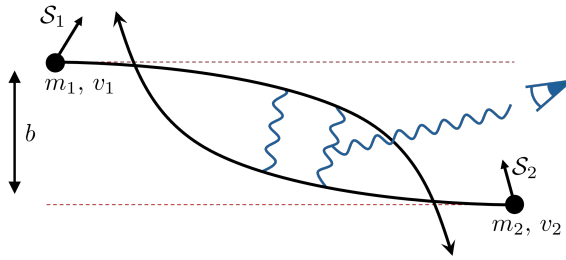


Figure 1: The scattering process of two massive compact objects that emits gravitational radiation. The scattering is mediated by the exchange of gravitational waves shown in blue. The initial masses, velocities and spins are indicated.

objects as black holes for simplicity.

In the remainder of this section, we set up our notation and conventions for the kinematic variables which are used to express all obtained scattering observables. We are

working in the mostly-minus metric signature, such that the asymptotic flat-space metric is given by

$$\eta_{\mu\nu} = \eta^{\mu\nu} = \text{diag}(1, -1, -1, -1) . \quad (2.1)$$

We consider a generic scattering process of n compact objects, such as black holes, which produces Bremsstrahlung with momentum k ,

$$(m_1 v_1, \dots, m_n v_n) \quad \rightarrow \quad (m_1 v_1 - q_1, \dots, m_n v_n - q_n, k) , \quad (2.2)$$

where we associate a mass m_i , a velocity v_i and a momentum exchange q_i to each black hole. The velocities are normalized as $v_i^2 = 1$ and momentum conservation relates the momentum of the emitted gravitational radiation k to the exchanged momenta q_i via

$$k = \sum_{i=1}^n q_i . \quad (2.3)$$

Next, we define kinematic invariants that parameterize the aforementioned scattering processes, following the conventions in ref. [120],

$$\omega_i = v_i \cdot k , \quad \omega_{ij} = v_i \cdot q_j , \quad q_i^2 , \quad q_{ij}^2 = (q_i + q_j)^2 , \quad y_{ij} = v_i \cdot v_j , \quad (2.4)$$

which are subject to the following constraints

$$\omega_i = \sum_{j=1}^n \omega_{ij} , \quad \omega_{ii} = 0 , \quad k^2 = \left(\sum_i q_i \right)^2 = \sum_{i < j} q_{ij}^2 - (n-2) \sum_{i=1}^n q_i^2 = 0 . \quad (2.5)$$

The classical amplitudes in the PM expansion are polynomial in the masses m_i of the compact objects and one can obtain their dependence directly from diagrammatic rules, as will be discussed below. Consequently, we can omit the m_i parameters in most computations. We do not use Gram-determinant identities to eliminate momentum redundancies which originate from the four dimensionality of spacetime, instead we assume general d -dimensional external momenta.

In this paper, we focus on two cases: two-body scattering ($n = 2$) and three-body scattering ($n = 3$). For the binary system there are only 5 variables,

$$\omega_1 , \quad \omega_2 , \quad q_1^2 , \quad q_2^2 , \quad y \equiv y_{12} . \quad (2.6)$$

For three-body scattering, we write our results in terms of the following 14 variables

$$\begin{aligned} &\omega_{ij} \quad \text{for } i, j = 1, 2, 3 \quad \text{and } i \neq j , \\ &y_{ij} , \quad q_{ij} \quad \text{for } i, j = 1, 2, 3 \quad \text{and } i < j , \\ &q_1^2 \quad \text{and } q_2^2 . \end{aligned} \quad (2.7)$$

In position space, the sources' initial trajectories will be the straight worldlines,

$$x_i^\mu(\tau) = b_i^\mu + \tau v_i^\mu , \quad (2.8)$$

which depend on the velocities v_i and the impact parameters b_i . Here τ is the proper time of the moving object. Finally, the objects' initial spin will be denoted by a rank-two tensor, \mathcal{S}_i^{ab} , which in turn is related to the classical spin vector

$$\mathcal{S}_i^a = \frac{1}{2} \epsilon^a_{bcd} v_i^b \mathcal{S}_i^{cd}, \quad (2.9)$$

with the convention $\epsilon^{0123} = 1$. We want to stress that the spin vectors \mathcal{S}_i^a in the WQFT are defined in their respective inertial frames [158] corresponding to v_i^b . This choice of reference frame matches the commonly chosen frame in the scattering-amplitude approach. Throughout our computation we impose the covariant spin-supplementary condition,

$$\mathcal{S}_i^{ab} v_{ia} = 0, \quad (2.10)$$

to uniquely specify the spin variables [158, 159]. Finally, it will often be useful to group a mass factor with the associated spin vector,

$$a_i^c = \frac{\mathcal{S}_i^c}{m_i}, \quad (2.11)$$

to emphasize the parameter dependences. The vectors a_i have the dimension of length and its norm $|a_i|$ corresponds to the ring radius of the rotating black hole.

For later convenience, we also introduce the following integral measures

$$\int_{\omega} \equiv \int_{-\infty}^{\infty} \frac{d\omega}{2\pi}, \quad \int_k \equiv \int \frac{d^d k}{(2\pi)^d}, \quad (2.12)$$

and the shorthand,

$$\hat{\delta}(x) = 2\pi\delta(x). \quad (2.13)$$

At last, we define the d -dimensional physical-state projector $P_{\mu\nu\rho\sigma}$ for the gravitational field as

$$P_{\mu\nu\rho\sigma} = \frac{1}{2} \left[\eta_{\mu\rho}\eta_{\sigma\nu} + \eta_{\mu\sigma}\eta_{\rho\nu} - \frac{2}{d-2}\eta_{\mu\nu}\eta_{\rho\sigma} \right]. \quad (2.14)$$

3 Waveforms from the worldline QFT formalism

We study the radiation emitted during the encounter of two spinning black holes by using the worldline quantum field theory (WQFT) approach [120–123]. The formalism has been extended [142, 160] to obtain the leading-order waveforms up to quadratic spin effects [140, 142], and was recently further generalized [161] to include higher-spin contributions. However, in this work we use a simplified supersymmetric variant [142, 160] suitable for obtaining spin-squared effects. In the following section, we review the main ideas of the WQFT approach for spinning sources. In particular, we provide a detailed elaboration on extracting the classical gravitational waveform in terms of many-body scattering diagrams.

3.1 The worldline theory and weak-field expansion

To describe black-hole scattering, we let N massive spinning bodies interact gravitationally

$$S = S_{\text{EH}} + S_{\text{gf}} + \sum_{i=1}^N S_i , \quad (3.1)$$

where the Einstein-Hilbert action S_{EH} is given by

$$S_{\text{EH}} = -\frac{2}{\kappa^2} \int d^4x \sqrt{|g|} R , \quad (3.2)$$

with $g = \det(g_{\mu\nu})$ and the Ricci scalar is defined by $R = R^\rho_{\mu\rho\nu} g^{\mu\nu}$. We will assume weak gravitational fields, such that one can expand the spacetime metric in a fluctuation $h_{\mu\nu}$ around flat space via

$$g_{\mu\nu}(x) \equiv \eta_{\mu\nu} + \kappa h_{\mu\nu}(x) , \quad (3.3)$$

where $\kappa = \sqrt{32\pi G}$, which is written in terms of the Newton constant G_N using $G = \hbar G_N / c^3$. The gauge fixing-term $S_{\text{gf}} = \int d^4x \eta_{\mu\nu} f^\mu f^\nu$ is used to impose the de Donder gauge, $f^\nu = \partial_\mu h^{\mu\nu} - \frac{1}{2} \partial^\nu h^\mu{}_\mu = 0$. Up to quadratic order in spin, the dynamics of a spinning massive body can be described by the worldline action [160]

$$S_i = -m_i \int d\tau \left[\frac{1}{2} g_{\mu\nu} \dot{x}_i^\mu \dot{x}_i^\nu + i \bar{\psi}_{i,a} \frac{D\psi_i^a}{D\tau} + \frac{1}{2} R_{abcd} \bar{\psi}_i^a \psi_i^b \bar{\psi}_i^c \psi_i^d \right] , \quad (3.4)$$

where $\dot{x}^\mu \equiv \partial x^\mu / \partial \tau$ and the covariant derivative is defined via $\frac{D\psi_i^a}{D\tau} = \dot{\psi}_i^a + \dot{x}^\mu \omega_\mu^{ab} \psi_{i,b}$ with the spin connection ω_μ^{ab} . To treat the fermionic degrees of freedom we have introduced the Vielbein $e_\mu^a(x)$, which is defined through the relation

$$g_{\mu\nu}(x) = e_\mu^a(x) e_\nu^b(x) \eta_{ab} . \quad (3.5)$$

Here the Roman letters are associated to the orthonormal tangent space related to the curved spacetime denoted by Greek indices. In the asymptotic flat spacetime, where we assume tangent and coordinate spaces to be aligned, we stop distinguishing Greek and Roman indices. The spin connection is linked to the Christoffel symbols by

$$\omega_\mu^{ab} \equiv e_\nu^a \left(\partial_\mu e^{\nu b} + \Gamma_{\mu\lambda}^\nu e^{\lambda b} \right) . \quad (3.6)$$

The dynamical variables are the trajectories $x_i^\mu(\tau)$ and the Grassmann worldline fields $\psi^a(\tau)$ and $\bar{\psi}^a(\tau)$. The interaction term including the Riemann tensor requires the Vielbein fields (3.5) to relate spacetime- to tangent-space indices.

To describe the scattering of black holes, we expand the trajectories around their initial configuration and wish to obtain the back reaction to the metric and the paths in perturbation theory. We therefore parameterize the paths via

$$x_i^\mu(\tau) = b_i^\mu + v_i^\mu \tau + z_i^\mu(\tau) , \quad (3.7)$$

where b_i is the impact parameter of particle i and v_i its initial velocity. (The initial momentum of the massive object is $p_j = m_j v_j$.) Finally, z_i represents the perturbation around

the background trajectory and is a new dynamical field, for which we impose the initial condition $z_i(-\infty) = 0$. Furthermore, the Grassmann fields are also expanded around the background

$$\psi_i^a(\tau) = \Psi_i^a + \phi_i^a(\tau), \quad (3.8)$$

with the perturbation $\phi_i^a(\tau)$. We require the field fluctuations to vanish in the infinite past, i.e. $\phi_i^a(-\infty) = 0$. The constant part, Ψ_i^a is related to the classical spin tensor [160]

$$\mathcal{S}_i^{ab} = -2im_i \bar{\Psi}_i^{[a} \Psi_i^{b]}, \quad (3.9)$$

where we used the following (anti-)symmetrization

$$x^{[a} y^{b]} \equiv \frac{1}{2} (x^a y^b - x^b y^a) \quad \text{and} \quad x^{(a} y^{b)} \equiv \frac{1}{2} (x^a y^b + x^b y^a). \quad (3.10)$$

The parameters b_i , v_i and \mathcal{S}_i will set the initial conditions of a scattering process.

Working in the perturbative weak-field regime, the inverse metric $g^{\mu\nu}$ and the determinant of the metric are expanded in κ ,

$$g^{\mu\nu} = \eta^{\mu\nu} - \kappa h^{\mu\nu} + \kappa^2 h^{\mu\lambda} h^\nu{}_\lambda - \kappa^3 h^{\mu\lambda} h_{\lambda\sigma} h^{\sigma\nu} + \mathcal{O}(\kappa^4), \quad (3.11)$$

$$\begin{aligned} \sqrt{|g|} &= 1 + \frac{\kappa}{2} h + \frac{\kappa^2}{8} (h^2 - 2h_{\mu\nu} h^{\mu\nu}) \\ &+ \frac{\kappa^3}{48} (h^3 - 6h h^{\mu\nu} h_{\mu\nu} + 8h^{\mu\nu} h_{\nu\lambda} h^\lambda{}_\mu) + \mathcal{O}(\kappa^4), \end{aligned} \quad (3.12)$$

where $h \equiv h^\mu{}_\mu$. Furthermore, we need the expansion of the covariant derivative ∇_μ , for which the required Christoffel symbols $\Gamma_{\mu\nu}^\lambda$ are expanded as

$$\Gamma_{\mu\nu}^\lambda = \frac{\kappa}{2} (\eta^{\lambda\omega} - \kappa h^{\lambda\omega} + \kappa^2 h^{\lambda\sigma} h_\sigma{}^\omega) (\partial_\mu h_{\omega\nu} + \partial_\nu h_{\mu\omega} - \partial_\omega h_{\mu\nu}) + \mathcal{O}(\kappa^4). \quad (3.13)$$

To treat spin, we must also expand the Vielbein e_μ^a and the spin-connection ω_μ^{ab} , which up to third order read

$$e_\mu^a = \eta^{a\nu} \left(\eta_{\mu\nu} + \frac{\kappa}{2} h_{\mu\nu} - \frac{\kappa^2}{8} h_{\mu\rho} h^\rho{}_\nu + \frac{\kappa^3}{16} h_{\mu\rho} h^\rho{}_\sigma h^\sigma{}_\nu \right) + \mathcal{O}(\kappa^4), \quad (3.14)$$

$$\begin{aligned} \omega_\mu^{ab} &= -\kappa \partial^{[a} h_{\mu}^{b]} - \frac{\kappa^2}{2} h^{\nu[a} \left(\partial^{b]} h_{\mu\nu} - \partial_\nu h_{\mu}^{b]} + \frac{1}{2} \partial_\mu h_{\nu}^{b]} \right) \\ &- \frac{\kappa^3}{8} h^{\nu[a} \left(2h^{b]\rho} \partial_\nu h_{\mu\rho} - 2h_\nu{}^\rho \partial_\mu h_{\rho}^{b]} + 3h_\nu{}^\rho \partial_\rho h_{\mu}^{b]} - 3h_\nu{}^\rho \partial^{b]} h_{\mu\rho} \right) + \mathcal{O}(\kappa^4). \end{aligned} \quad (3.15)$$

Finally, the inverse Vielbein obtains the expansion

$$e_a^\mu = \eta^{\mu\nu} \left(\eta_{a\nu} - \frac{\kappa}{2} h_{a\nu} + \frac{3\kappa^2}{8} h_{\nu\rho} h^\rho{}_a - \frac{5\kappa^3}{16} h_{\nu\rho} h^\rho{}_\sigma h^\sigma{}_a \right) + \mathcal{O}(\kappa^4). \quad (3.16)$$

3.2 The gravitational waveform

Having defined the dynamics of the system, we now discuss the gravitational-wave observable which we wish to compute. During a scattering event, the two black holes accelerate

and emit gravitational radiation which is measured in observatories. We want to compute the radiation's waveform at large distance $|\mathbf{r}| \gg b$ from the scattering objects. The radiated metric perturbation $\kappa h^{\mu\nu}$ of two scattering black holes is obtained by solving the classical Einstein field equations perturbatively in the Newton coupling G_N (or equivalently κ). The waveform h_s^∞ is then identified as the coefficient of the leading contribution in the $1/|\mathbf{r}|$ expansion of the metric fluctuation,

$$\kappa \varepsilon_s^{\mu\nu} h_{\mu\nu}^{\text{cl}}(r; \mathcal{S}, p, b) \Big|_{|\mathbf{r}| \rightarrow \infty} = \frac{1}{|\mathbf{r}|} h_s^\infty(t - |\mathbf{r}|, \mathbf{n}; \mathcal{S}, p, b) + \mathcal{O}(|\mathbf{r}|^0), \quad (3.17)$$

where $k = \omega \hat{k} = \omega(1, \mathbf{n})$, with $\mathbf{n} = \mathbf{r}/|\mathbf{r}|$. The label $s \in \{\times, +\}$ specifies the polarization $\varepsilon_s^{\mu\nu}$ of the radiation, and the parameters \mathcal{S} , p and b specify the objects' spin, their initial momentum and impact parameter, respectively. The time-domain waveform $h_s^\infty(t - |\mathbf{r}|, \mathbf{n}; \mathcal{S}, p, b)$ is related to the momentum-space waveform by the Fourier transform,

$$h_s^\infty(t - |\mathbf{r}|, \mathbf{n}; \mathcal{S}, p, b) = \frac{\kappa}{4\pi} \int_0^\infty \frac{d\omega}{2\pi} e^{-i\omega(t-|\mathbf{r}|)} \left[k^2 \varepsilon_s^{\mu\nu}(k) h_{\mu\nu}^{\text{cl}}(k; \mathcal{S}, p, b) \right]_{k=\omega \hat{k}} + c.c., \quad (3.18)$$

of the on-shell momentum-space metric fluctuation $h_{\mu\nu}(k; \mathcal{S}, p, b)$. (To simplify notation, we will often suppress the initial-data and denote it by $h_{\mu\nu}(k)$.) Consequently, the central quantity we need to obtain is the on-shell momentum-space waveform,

$$O = k^2 \varepsilon_s^{\mu\nu}(k) h_{\mu\nu}^{\text{cl}}(k; \mathcal{S}, p, b) \Big|_{k=\omega \hat{k}}. \quad (3.19)$$

We will compute the quantity (3.19) in a perturbative expansion,

$$O = \sum_{i,j,k,l \geq 0} O^{ijkl} \left(\frac{r_{s,1}}{b} \right)^i \left(\frac{r_{s,2}}{b} \right)^j \left(\frac{\mathcal{S}_1/m_1}{b} \right)^k \left(\frac{\mathcal{S}_2/m_2}{b} \right)^l, \quad (3.20)$$

where the expansion (3.20) is in terms of the ring radius $a_i = S_i/m_i$ (2.11). We will focus on contributions at next-to-leading order in the gravitational coupling and up to second order in spin, i.e. $\mathcal{O}(G^3 \mathcal{S}^2)$ using the G -dependence of $r_{s,i} \sim G$ and the spin \mathcal{S} as convenient counting parameters.

3.3 Classical metric from worldline QFT

The classical gravitational Bremsstrahlung is emitted as a non-trivial metric perturbation, which we compute perturbatively in the gravitational coupling G and spin \mathcal{S} . We choose to work in a worldline QFT setup [121, 123] to obtain a diagrammatic approach based on modern field-theory methods. This approach was already successfully applied to the LO $\mathcal{O}(G^2 \mathcal{S}^2)$ waveforms including spin corrections [120, 160], and we will focus on the NLO corrections at $\mathcal{O}(G^3)$. Alternative field-theory approaches have provided the waveform observable at LO at $\mathcal{O}(G^2)$ including all-order in spin corrections [143–145, 162], and at NLO at $\mathcal{O}(G^3)$ [146–150, 157] including linear-in-spin contributions [150]. We will apply the latter type of approach for validation for which further details can be found in section 5.

In the worldline QFT approach the metric fluctuation is determined from the "in-in" one-point function $\langle h_{\mu\nu}(k) \rangle_{\text{in-in}}$ of the Keldysh-Schwinger path integral [163, 164]. The classical field $h_{\mu\nu}^{\text{cl}}$ is obtained by omitting quantum corrections,

$$h_{\mu\nu}^{\text{cl}}(k) = \langle h_{\mu\nu}(k) \rangle_{\text{in-in}} \Big|_{\text{classical}}. \quad (3.21)$$

In the following, we will closely follow the path-integral formulation of ref. [121], which we refer to for details on the formalism. Here, we collect the key points of the method:

1. In the classical limit, the expectation value $\langle h_{\mu\nu}(k) \rangle_{\text{in-in}}$ is obtained from connected tree-level diagrams of the worldline theory coupled to gravity (3.1).
2. As opposed to a standard Feynman-diagram computation, the adjustment for computing the "in-in" one-point function amounts to using retarded propagators instead of Feynman propagators.
3. The formalism provides a mechanism to assign the retarded propagators matching the causality of the process. The latter aspect is simple to account for in tree-level diagrams, which have a well defined causality flow from sources to the final emitted gravitational radiation.
4. The relevant vertex rules for the Keldysh-Schwinger path integral are equivalent to the vertex rules derived from the worldline (3.4) and Einstein-Hilbert action (3.2) [121].

We thus have available a simple diagrammatic approach to obtain the classical metric fluctuation $h_{\mu\nu}^{\text{cl}}(k)$.

3.4 Feynman rules

In the WQFT approach we promote the perturbation fields $z_i^\mu(\tau)$, $\phi_i^a(\tau)$ and $h_{\mu\nu}(x)$ to quantum fields. The fields are used in their momentum-space variants,

$$z_i^\mu(\tau) = \int_{\omega} e^{i\omega\tau} z_i^\mu(-\omega), \quad \phi_i^\mu(\tau) = \int_{\omega} e^{i\omega\tau} \phi_i^\mu(-\omega), \quad h_{\mu\nu}(x) = \int_k e^{ik \cdot x} h_{\mu\nu}(-k), \quad (3.22)$$

which allows us to derive Feynman rules. Given that in the worldline action S_i the graviton field implicitly depends on the trajectory, it must be expanded using

$$\begin{aligned} h_{\mu\nu}(x_i(\tau)) &= \int_k e^{ik \cdot (b_i + v_i \tau + z_i(\tau))} h_{\mu\nu}(-k) \\ &= \sum_{n=0}^{\infty} \frac{i^n}{n!} \int_k e^{ik \cdot (b_i + v_i \tau)} [k \cdot z_i(\tau)]^n h_{\mu\nu}(-k) \\ &= \sum_{n=0}^{\infty} \frac{i^n}{n!} \int_{k, \omega_1, \dots, \omega_n} e^{ik \cdot b_i} e^{i(k \cdot v_i + \sum_{j=1}^n \omega_j) \tau} \left(\prod_{j=1}^n k \cdot z_i(-\omega_j) \right) h_{\mu\nu}(-k), \end{aligned} \quad (3.23)$$

which leads to polynomial interaction terms. Due to this dependence on the trajectory, we will obtain vertices with an arbitrary numbers of z -fields from eq. (3.4). In contrast,

the number of ϕ -fields in a given vertex is constrained to be at most four due to the third term in the worldline action (3.4). Furthermore, plugging the above expressions into the action allows to integrate out the proper time τ , which gives rise to energy-conserving delta functions $\delta(k \cdot v_i + \sum_{j=1}^n \omega_j)$. The Feynman rules can now be extracted by considering the path integral over the fluctuating fields with the action of (3.1) and taking functional derivatives. For details on the Feynman vertices we refer the reader to refs. [120, 160] and appendix A.

We conclude this section by collecting the required propagator conventions. The retarded momentum-space graviton propagator is given by

$$h_{\mu\nu} \xrightarrow{k} h_{\rho\sigma} = i \frac{P_{\mu\nu\rho\sigma}}{(k^0 + i\epsilon)^2 - \mathbf{k}^2} = i \frac{P_{\mu\nu\rho\sigma}}{k^2 + i\epsilon \operatorname{sgn}(k^0)}, \quad (3.24)$$

with

$$\operatorname{sgn}(x) \equiv \begin{cases} 1 & x > 0 \\ 0 & x = 0 \\ -1 & x < 0 \end{cases}. \quad (3.25)$$

The propagator for the z -field is

$$z_\mu \xrightarrow{\omega} z_\nu = -i \frac{\eta_{\mu\nu}}{m_i(\omega + i\epsilon)^2}, \quad (3.26)$$

and the propagators for the ϕ -field and $\bar{\phi}$ -field are

$$\phi_\mu \xrightarrow{\omega} \bar{\phi}_\nu = \frac{-i \eta_{\mu\nu}}{m_i(\omega + i\epsilon)}, \quad \bar{\phi}_\mu \xrightarrow{\omega} \phi_\nu = \frac{-i \eta_{\mu\nu}}{m_i(\omega + i\epsilon)}. \quad (3.27)$$

In the diagrammatic representation of the propagators we indicate the momentum (frequency) definition with an additional arrow, while the arrow on the diagram line itself specifies the causality flow, i.e. if momentum arrows are aligned the signs of k^0 (ω) and $i\epsilon$ match in eqns. (3.24), (3.26), and (3.27). We suppress the conventional arrow for fermion lines, since both propagators are equivalent.

To fix our conventions we also give the position-space Green functions for the metric fluctuation,

$$h_{\mu\nu}(x_1) \xrightarrow{h_{\rho\sigma}(x_2)} = \int_k \frac{i P_{\mu\nu\rho\sigma}}{(k^0 + i\epsilon)^2 - \mathbf{k}^2} e^{-ik \cdot (x_2 - x_1)}, \quad (3.28)$$

and the fields $z(\tau)$,

$$z_\mu(\tau_1) \xrightarrow{z_\nu(\tau_2)} = \int_\omega \frac{-i \eta_{\mu\nu}}{m_i(\omega + i\epsilon)^2} e^{-i\omega(\tau_2 - \tau_1)}, \quad (3.29)$$

and similar for the Grassmann fields. The Green functions have non-vanishing (retarded) support for $x_2^0 > x_1^0$ and $\tau_2 > \tau_1$, respectively.

3.5 Classical amplitudes

The one-point function $\langle h^{\mu\nu} \rangle_{\text{in-in}}$ has a diagrammatic expansion in terms of WQFT Feynman diagrams, which we now analyse to simplify their computation. Its schematic form is depicted in fig. 2a, where a number of worldlines (dotted lines) interact via graviton exchange to produce the metric fluctuation $h_{\mu\nu}^{\text{cl}}$. The external graviton leg represents a graviton-field propagator. The worldlines support the dynamical fields z_i and the fermionic fields ϕ_i^a which propagate and interact. The propagating worldline fields are displayed by solid lines (see e.g. diagrams fig. 4). The interaction vertices may include the background data v_i and Ψ_i^a as well as the masses m_i . In fig. 2b, we show an exemplary n-body contribution to the expectation value at the leading order in perturbation theory. Here n worldlines emit a graviton field each, which produce the final classical metric fluctuation with momentum k . The diagram contributes at order κ^{2n-1} and is proportional to the mass monomial $(m_1 \cdots m_n)$, which is manifest from the κm_i dependence of the graviton-worldline vertex (A.3) and the κ^{n-1} dependence of the (n+1)-point graviton vertex. Diagrams may have additional mass dependence linked to spin vectors only; explicitly this dependence is of the form $a_i = (S_i/m_i)$, as again manifest in the Feynman rules (see appendix A). Below, we find it convenient to write diagrams in terms of the ring radius a_i . In this way, the diagrams have a homogeneous scaling in the mass parameters.

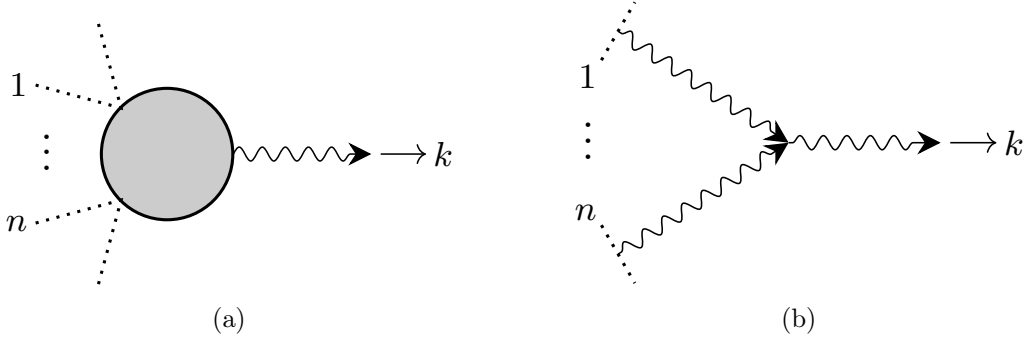


Figure 2: Left: Diagrammatic representation of the required amplitude for the gravitational waveform. Right: An example diagram contributing to the amplitude. Dotted lines denote background fields Ψ_i^a , while wavy lines denote graviton field $h_{\mu\nu}$.

In a waveform computation, we do not require the off-shell metric field $h_{\mu\nu}^{\text{cl}}$ itself, since a number of simplifications appear in expression (3.19): First of all, the waveform computation requires to multiply the classical field with the inverse propagator k^2 . Furthermore, we require the classical field contracted with the polarization state $\varepsilon_s^{\mu\nu}$. Finally, it is sufficient to consider the on-shell ($k^2 = 0$) graviton-field momentum. We refer to this amputated one-point function as the scattering amplitude in impact-parameter space and we use the notation,

$$\widehat{\mathcal{M}}_s \equiv \kappa k^2 \varepsilon_s^{\mu\nu} h_{\mu\nu}^{\text{cl}}(k). \quad (3.30)$$

The object contains an infinite sum of WQFT diagrams, which we now wish to organize, so that we can tackle them.

The diagrammatic organisation of the WQFT approach makes manifest a number of useful properties [120, 121, 134, 142, 160]. To exploit these, it is useful to introduce the notion of a generating amplitude, which is the contribution to $\widehat{\mathcal{M}}_s$ from precisely n background worldlines,

$$\widehat{\mathcal{M}}_s^n(1, 2, \dots, n) = \widehat{\mathcal{M}}_s \Big|_{n \text{ sources}}. \quad (3.31)$$

The integer arguments specify the type of participating worldlines, and refer to the subscript of the worldline actions S_i of eq. (3.4). We now discuss the properties of this generating object in more detail.

Mass and coupling dependence: The generating amplitudes have a specific mass-scaling and perturbative order,

$$\widehat{\mathcal{M}}_s^n(1, 2, 3, \dots, n) \sim G^n \prod_{i=1}^n m_i. \quad (3.32)$$

For this scaling to hold we group mass parameters with the spin vectors $a_i = \mathcal{S}_i/m_i$ and consider the expressions to be functions of the ring radii a_i . In this way the generating amplitudes simultaneously make manifest the self-force expansion as well as the PM expansion [135]. An example diagram contributing to $\widehat{\mathcal{M}}_s^n(1, 2, \dots, n)$ is displayed in fig. 2b.

Symmetry: The amplitude $\widehat{\mathcal{M}}_s^n(1, 2, \dots, n)$ is symmetric under the exchange of sources,

$$\widehat{\mathcal{M}}_s^n[\sigma_n(1), \sigma_n(2), \dots, \sigma_n(n)] = \widehat{\mathcal{M}}_s^n(1, 2, 3, \dots, n), \quad (3.33)$$

where σ_n denotes a permutation of n objects. This symmetry allows to reduce the number of diagrams which need to be computed. In particular, one can symmetrize over individual diagrams to obtain an amplitude.

Generating amplitudes: The very same n -worldline diagrams may as well be used to obtain higher-order (classical) gravitational corrections. In fact, by inspection one finds that identifying worldlines to originate from the same action S_i (with parameters m_i , b_i and v_i), leading-order diagrams can be transcribed to higher-order contributions [120, 155]. Consequently, when computing an n -body waveform, we obtain as well the $\mathcal{O}(G^m)$ corrections to the $(n - m)$ -body waveform. To give an example, the amplitude

$$\widehat{\mathcal{M}}_s^2(1, 2) \sim G^2 m_1 m_2 \quad (3.34)$$

contributes at leading order to the two-body interaction, while the amplitudes

$$\widehat{\mathcal{M}}_s^3(1, 2, 2) \sim G^3 m_1 m_2^2 \quad \text{and} \quad \widehat{\mathcal{M}}_s^3(1, 1, 2) \sim G^3 m_1^2 m_2 \quad (3.35)$$

contribute at the next-to-leading order G^3 . By iteration, all higher-order corrections arise from the generating amplitudes (3.31), which justifies this notion.

Static background: Identifying all background data with the ones of a single source,

$$\widehat{\mathcal{M}}_s^n(1, 1, \dots, 1) \sim G^n m_1^n \quad (3.36)$$

gives static contributions to the metric, which are the leading term in the waveform's self-force expansion. Representative diagrams obtained from this identification are shown in fig. 3. Such diagrams give the perturbative expansion of a black-hole metric translated by

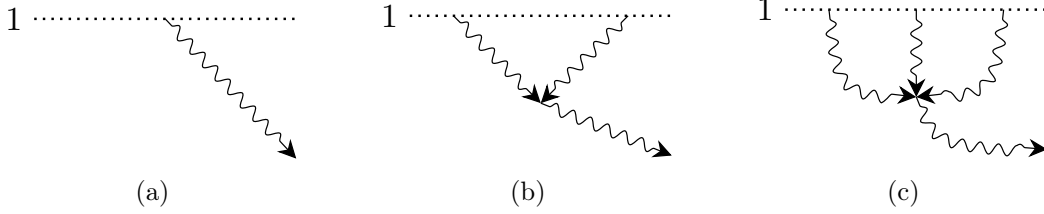


Figure 3: Example diagrams corresponding to corrections of the static background at different orders in κ . Dotted lines represent background fields Ψ_i^a , and wavy lines represent graviton fields $h_{\mu\nu}$.

the impact parameter b_1 (see e.g. [165–167]), and we will discuss them further below.

Sum of contributions: Putting the generating amplitudes back together to obtain the impact-parameter space amplitude, we have to sum up generating amplitudes of various multiplicities. For concreteness, we state this for two-body scattering up to order G^3 ,

$$\begin{aligned} \widehat{\mathcal{M}}_s = & \widehat{\mathcal{M}}_s^1(1) + \widehat{\mathcal{M}}_s^1(2) + \widehat{\mathcal{M}}_s^2(1, 1) + \widehat{\mathcal{M}}_s^2(1, 2) + \widehat{\mathcal{M}}_s^2(2, 2) \\ & + \widehat{\mathcal{M}}_s^3(1, 1, 1) + \widehat{\mathcal{M}}_s^3(1, 1, 2) + \widehat{\mathcal{M}}_s^3(1, 2, 2) + \widehat{\mathcal{M}}_s^3(2, 2, 2) + \mathcal{O}(G^4). \end{aligned} \quad (3.37)$$

It is important to note that only connected diagrams contribute, since disconnected diagrams are excluded in the classical waveform observable by definition in the worldline QFT. In a field-theory approach connected worldline diagrams may appear as disconnected field-theory diagrams [154]. Thus the notion of diagram topology differs in the two approaches. An example for this are the static background contributions mentioned above.

Feynman integrals: The general form of a WQFT diagram closely resembles the one of Feynman amplitudes. In particular, a single diagram gives rise to a momentum integral in dimensional regularization, with a rational integration kernel and delta-function constraints. A given diagram of the generating amplitude $\widehat{\mathcal{M}}_s^n$ takes the form

$$D_{n,\gamma} = \kappa^{2n-1} \left(\prod_{i=1}^n m_i \right) \int d\mu_n(1, \dots, n) \frac{N_\gamma}{\prod_{i \in P(\gamma)} \rho_i}, \quad (3.38)$$

where ρ_i denotes retarded propagators labeled by i in the set $P(\gamma)$ of all edges of the diagram γ and N_γ is the polynomial numerator emerging from the Feynman rules. The measure factor arises from energy conservation along the worldlines and momentum conservation in

the graviton interactions. It is given by,

$$d\mu_n(1, \dots, n) \equiv \left[\prod_{j=1}^n \frac{d^d q_j}{(2\pi)^d} e^{i q_j \cdot b_j} \hat{\delta}(v_j \cdot q_j) \right] \hat{\delta}^{(d)} \left(k - \sum_{j=1}^n q_j \right), \quad (3.39)$$

where we introduced the shorthand notation $\hat{\delta}(x) \equiv 2\pi\delta(x)$. The q_i 's refer to the sum of all graviton momenta that are connected to background i . A set of example diagrams is shown e.g. in fig. 4. Each diagram has a specific overall mass scaling and dependence on the gravitational coupling κ .

The main distinction of a WQFT integral (3.38) from a Feynman integral is the Fourier phase factor depending on the impact parameters b_i . It is convenient to split the integration into a Fourier integration and a remaining standard Feynman amplitude $\mathcal{M}_s^{n,g}$. For the generating amplitudes (3.31), which include n distinct sources, the Feynman amplitude is obtained by dropping the measure altogether. For contributions with identified sources, as we discuss below, the integration includes Fourier integrals as well as momentum integrals over rational integration kernels. Separating the Fourier integration is technically convenient, since otherwise an extension of the standard Feynman integral calculus is required [168]. Conceptually, this split makes sense, since the momentum-space amplitude matches the ones obtainable in the field-theory approach (see section 5).

We now introduce the momentum-space amplitudes. We start with the generating amplitudes and define the momentum-space generating amplitude $\mathcal{M}_s^{n,g}(1, 2, \dots, n)$ implicitly through

$$\widehat{\mathcal{M}}_s^n(1, \dots, n) = \int d\mu_n(1, \dots, n) \mathcal{M}_s^{n,g}(1, \dots, n), \quad (3.40)$$

assuming distinct sources and thus distinct integer labels.

The treatment of integration differs for amplitudes with identified sources. In this case, not all impact parameters b_i are distinct and we can perform a linear change of integration variables q_i to isolate integrals that do not affect the Fourier phases at all,

$$d\mu_n(i_1, \dots, i_{n-m}, 1, 2, \dots, m) \rightarrow d\mu_m(1, 2, \dots, m) \times \left[\prod_{j=1}^{n-m} \frac{d^d \ell_j}{(2\pi)^d} \hat{\delta}(v_{i_j} \cdot \ell_j) \right], \quad (3.41)$$

where $i_k \in \{1, \dots, m\}$. The phase-independent integration directions are denoted by ℓ_i and they match loop integration in the field-theory approach. We define momentum-space amplitudes by

$$\begin{aligned} & \mathcal{M}_s^n(i_1, \dots, i_{n-m}, 1, 2, \dots, m) \\ & \equiv \left[\prod_{j=1}^{n-m} \int \frac{d^d \ell_j}{(2\pi)^d} \hat{\delta}(v_{i_j} \cdot \ell_j) \right] \mathcal{M}_s^{n,g}(i_1, \dots, i_{n-m}, 1, 2, \dots, m), \end{aligned} \quad (3.42)$$

such that

$$\widehat{\mathcal{M}}_s^n(i_1, \dots, i_{n-m}, 1, 2, \dots, m) = \int d\mu_m(1, \dots, m) \mathcal{M}_s^n(i_1, \dots, i_{n-m}, 1, 2, \dots, m). \quad (3.43)$$

These momentum-space amplitudes are equivalent to field-theory loop amplitudes with some propagators being delta functions. In the argument, an ordered set of indices is sorted to the end and repeated indices $\{i_1, \dots, i_{n-m}\}$ are inserted in the beginning of the argument list in eqs. (3.41) to (3.43). When unambiguous, we will also treat the labels as symmetric arguments.

In the case of computing higher-order corrections to the two-body system, we will see that the resulting integrals are Feynman integrals. In the remainder of this section, we analyze which diagrams are required to extract the waveform at order $\mathcal{O}(G^3)$ and what integrals they will give rise to.

To give an example for these formal steps we consider the static background contributions. For these we identify all sources, say with the worldline one,

$$\{m_i, v_i, b_i, S_i\} \rightarrow \{m_1, v_1, b_1, S_1\}, \quad q_{i < n} \rightarrow \ell_i \quad \text{and} \quad q_n \rightarrow q_1 - \sum_{i=1}^{n-1} \ell_i, \quad (3.44)$$

in eq. (3.39). The measure factorizes as,

$$d\mu_n(1, \dots, n) = \int d\mu_1(1) \times \left[\prod_{i=1}^{n-1} \frac{d^d \ell_i}{(2\pi)^d} \hat{\delta}(\ell_i \cdot v_1) \right] \quad (3.45)$$

and we obtain the momentum-space amplitude,

$$\mathcal{M}_s^n(1, 1, \dots, 1) = \left[\prod_{j=1}^{n-1} \int \frac{d^d \ell_j}{(2\pi)^d} \hat{\delta}(v_1 \cdot \ell_j) \right] \mathcal{M}_s^{n,g}(1, \dots, 1), \quad (3.46)$$

which is an $(n-1)$ -loop contribution to the static background contributing at $\mathcal{O}(G^n)$. The impact-parameter amplitude is the Fourier transform,

$$\widehat{\mathcal{M}}_s^n(1, 1, \dots, 1) = \int d\mu_1(1) \mathcal{M}_s^n(1, 1, \dots, 1), \quad (3.47)$$

$$d\mu_1(1) = \frac{d^d q_1}{(2\pi)^d} e^{iq_1 \cdot b_1} \hat{\delta}(v_1 \cdot q_1) \hat{\delta}^{(d)}(k - q_1). \quad (3.48)$$

As we have hinted with the choice of variables names ℓ_i , $n-1$ of the integrals turn into Feynman-like integrals (albeit with retarded propagators). Representative diagrams obtained from this identification are shown in fig. 3. The remaining integration over q_1 corresponds to the Fourier transformation from momentum to impact parameter space. The delta functions enforce the zero-energy condition $v_1 \cdot k = 0$ and the diagrams yield only static metric fluctuations that are not detectable by gravitational-wave observatories.

3.6 Two-body scattering from seven-point trees

We now specialize the earlier methods to obtain the next-to-leading order corrections,

$$\mathcal{M}_s^3(1, 1, 2) \quad \text{and} \quad \mathcal{M}_s^3(1, 2, 2), \quad (3.49)$$

which contribute at $\mathcal{O}(G^3)$. We start by considering the generating amplitudes $\mathcal{M}_s^{3,g}(1,2,3)$ of the leading-order three-body black-hole scattering. The relevant diagrams at $\mathcal{O}(\kappa^5)$ are shown in fig. 4. We want to emphasize that the bold lines correspond to either z_i^μ , ϕ_i^a or $\bar{\phi}_i^a$ fields and all permutations of sources for each diagram have to be taken into account. We also do not consider disconnected diagrams, since they do not contribute to the classical waveform observable.

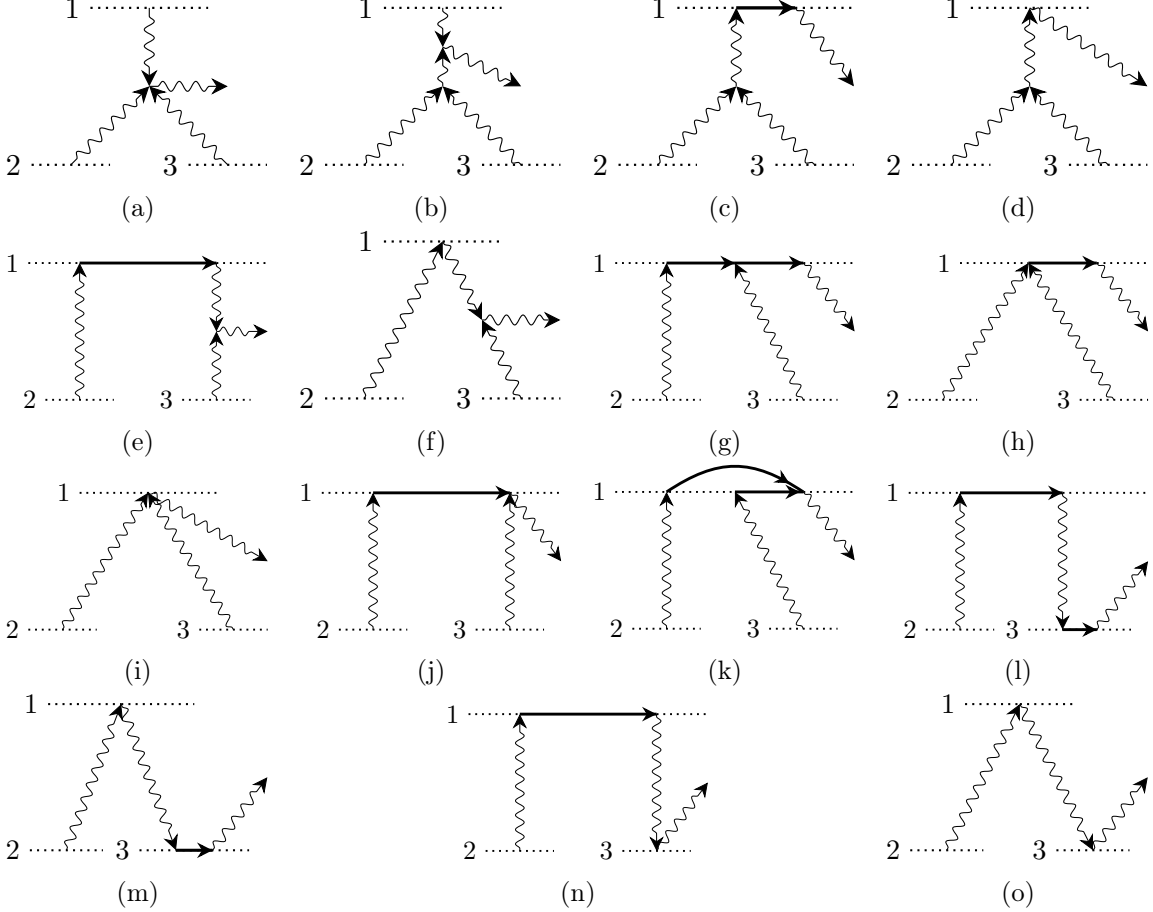


Figure 4: The diagrams contributing to the leading-order three-body waveform in the WQFT. Dotted lines represent background fields Ψ_i^a , wavy lines represent graviton fields $h_{\mu\nu}$ and bold black lines depict z_i^μ , ϕ_i^a and $\bar{\phi}_i^a$ fields. Arrows indicate the direction of momentum flow, relevant for the retarded propagators. The set of all diagrams is obtained by permuting the labels $(1,2,3) \rightarrow (\sigma(1), \sigma(2), \sigma(3))$.

The NLO correction to the binary scattering is recovered by identifying two of the background fields to be identical, as shown in fig. 5. The amplitudes' mass dependence $\mathcal{M}_s^3(1,1,2) \sim G^3 m_1^2 m_2$ and $\mathcal{M}_s^3(1,2,2) \sim G^3 m_1 m_2^2$ solely arises from the type of identification. Let us now focus on the $(m_1 m_2^2)$ part $\mathcal{M}_s^3(1,2,2)$ of the classical amplitude. ($\mathcal{M}_s^3(1,1,2)$ follows from relabeling.) Each diagram contributes multiple terms to the $(m_1 m_2^2)$ structure as all possible permutations of the identification of the background fields

have to be performed for each of the diagrams. In practice, we obtain all permutations of the indices $(1, 2, 3)$ for all diagrams shown in fig. 4 and then set

$$\{m_3, v_3, b_3, \mathcal{S}_3\} \rightarrow \{m_2, v_2, b_2, \mathcal{S}_2\} . \quad (3.50)$$

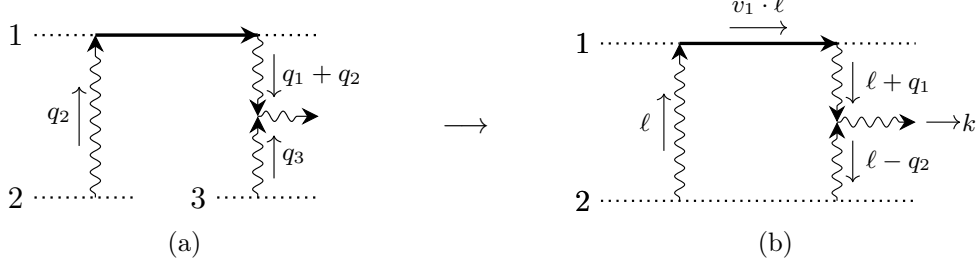


Figure 5: Diagram (a) with three distinct sources is relabeled ($3 \rightarrow 2$) to obtain diagram (b) involving two worldlines. While diagram (a) is a LO contribution to the gravitational exchange of three sources, diagram (b) contributes at NLO to the waveform of two scattering objects.

Next, we deal with the momentum integrals. In order to separate the Fourier integral we must find a parameterization of q_2 and q_3 , such that the total momentum emitted from the two worldline-2 contributions adds up to q_2 . This means the parameterization must fulfill $q_2 + q_3 \rightarrow q_2$. A family of such transformations is

$$q_2 \rightarrow \pm \ell + x q_2 , \quad q_3 \rightarrow (1 - x) q_2 \mp \ell . \quad (3.51)$$

Here x is a number that can, together with the sign of ℓ , be freely chosen. We will make use of this freedom to simplify the expressions of the emerging integrals. In particular, the choice is guided by the goal to obtain the following integration measure:

$$\int d\mu_3(1, 2, 3) \rightarrow \int d\mu_2(1, 2) \int \frac{d^d \ell}{(2\pi)^d} \hat{\delta}(\ell \cdot v_2) . \quad (3.52)$$

A suitable choice of x and the sign of ℓ depends on the specific diagrams under consideration and will be discussed in section 4.1. The identification procedure maps the tree-level diagram into a Feynman integral over a loop-momentum ℓ ,

$$\mathcal{M}_s^3(1, 2, 2) = \int \frac{d^d \ell}{(2\pi)^d} \hat{\delta}(v_2 \cdot \ell) \mathcal{M}_s^{3,g}(1, 2, 2) . \quad (3.53)$$

We now discuss the Feynman integral topologies which need to be computed.

Self-energy diagrams: Some identifications lead to self-energy contributions which we are allowed to omit. An example diagram is shown in fig. 6, which originates from the $(1, 2, 3) \rightarrow (3, 2, 1)$ permutation of diagram fig. 4n after identifying worldline 3 with worldline 2. Such diagrams naively appear to be divergent, since they contain a delta function

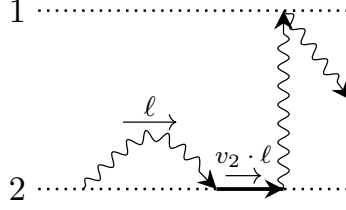


Figure 6: A self-energy diagram that does not contribute as it gives rise to scaleless integrals.

$\delta(v_2 \cdot \ell)$ as well as a propagator $i/(v_2 \cdot \ell + i\epsilon)$. After representing the delta functions as a difference of propagators

$$2\pi i \delta(v_2 \cdot \ell) = \frac{1}{v_2 \cdot \ell - i\epsilon} - \frac{1}{v_2 \cdot \ell + i\epsilon}, \quad (3.54)$$

we obtain scaleless integrals depending on a single propagator raised to higher power $1/(v_2 \cdot \ell + i\epsilon)^n$. Such integrals integrate to zero in dimensional regularization and we drop them in our calculation.

Integral topologies: Upon identification of background worldlines ($3 \rightarrow 2$) in the permutations $\{\sigma_3^i\}_{i=1,6}$ of $(1, 2, 3) \rightarrow (\sigma_3^i(1), \sigma_3^i(2), \sigma_3^i(3))$ of fig. 4, we encounter two integral families, defined by the pentagon diagram fig. 7a and its pinches, as we will now discuss. The general form of these pentagon integrals is

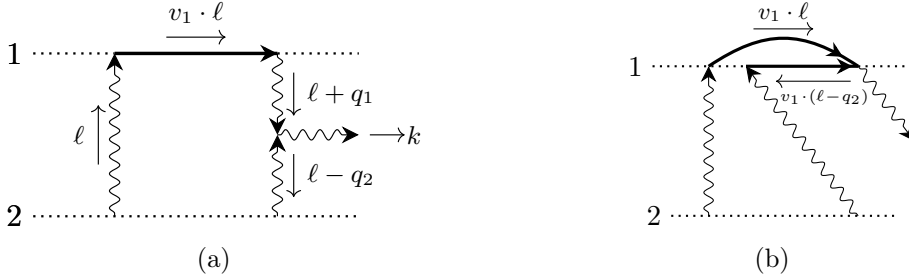


Figure 7: a) The parent topology of the $m_1 m_2^2$ sector of integrals. b) This topology has linearly dependent propagators for the z/ϕ -lines and can be reduced with the help of partial fractioning.

$$\mathcal{I}_{\vec{\nu}} = \int \frac{d^d \ell}{(2\pi)^d} \frac{1}{\rho_1^{\nu_1} \rho_2^{\nu_2} \rho_3^{\nu_3} \rho_4^{\nu_4}} \delta(\rho_5), \quad (3.55)$$

with $\vec{\nu} = \{\nu_1, \nu_2, \nu_3, \nu_4\}$ and

$$\begin{aligned} \rho_1 &= \ell^2 + i\epsilon \operatorname{sgn}(\ell^0), & \rho_2 &= v_1 \cdot \ell + i\epsilon, & \rho_3 &= (\ell + q_1)^2 + i\epsilon \operatorname{sgn}(\ell^0 + q_1^0) \\ \rho_4 &= (\ell - q_2)^2 - i\epsilon \operatorname{sgn}(\ell^0 - q_2^0), & \rho_5 &= v_2 \cdot \ell. \end{aligned} \quad (3.56)$$

While not originating directly from a propagator in a Feynman diagram, we include the ℓ -dependent delta function $\delta(\rho_5)$ from momentum conservation. Originally, it is associated to the measure (3.39), but is regrouped after identification of the background lines (3.41).

Most diagrams are obviously identified as pinches of the above pentagon. The only non-trivial case arises from identifications of fig. 4k and the topology is shown in fig. 7b. The corresponding topology is given by

$$\mathcal{I}' = \int \frac{d^d \ell}{(2\pi)^d} \frac{1}{\rho_1 \rho_2 \rho_6 \rho_4} \delta(\rho_5), \quad \text{with} \quad \rho_6 = v_1 \cdot (\ell - q_2) - i\epsilon. \quad (3.57)$$

In this topology, the propagators ρ_2 and ρ_6 associated with the z_i^μ or ϕ_i^a fields are linearly dependent. Their product can be simplified by partial fractioning,

$$\frac{1}{[v_1 \cdot \ell + i\epsilon][v_1 \cdot (\ell - q_2) - i\epsilon]} = -\frac{1}{v_1 \cdot q_2} \left[\frac{1}{[v_1 \cdot \ell + i\epsilon]} - \frac{1}{[v_1 \cdot (\ell - q_2) - i\epsilon]} \right]. \quad (3.58)$$

Inserting these expression we can express the pentagon integral \mathcal{I}' in terms of two box integrals of the pentagon family \mathcal{I} ,

$$\mathcal{I}' = -\frac{1}{v_1 \cdot q_2} \left[\mathcal{I}_{1,1,0,1} + \mathcal{I}_{1,1,0,1} \Big|_{\ell \rightarrow q_2 - \ell} \right]. \quad (3.59)$$

Similarly, pinches of \mathcal{I}' are mapped to the pentagon family of \mathcal{I} . Using integration-by-parts (IBP) relations [169–171] we can reduce all tensor integrals to scalar master integrals in the pentagon family. The second integral family (appearing in contributions of mass scaling $m_1^2 m_2$) is recovered from exchanging $(1 \leftrightarrow 2)$.

In summary, we require the integrands of $\mathcal{M}_s^{3,g}(1, 2, 3)$ as well as the integrals \mathcal{I} for the momentum-space amplitudes $\mathcal{M}_s^3(1, 2, 2)$ and $\mathcal{M}_s^3(1, 1, 2)$. We will turn to their computation next.

4 Waveform computation

In this section, we will describe the technical details of our computation of the spectral waveform. We will start by discussing the construction of the LO three-body integrand and explain the symmetrization and identification of the background fields. Afterwards, we elaborate on how we map this into higher-order corrections for the two-body waveform. Finally, we will discuss the evaluation of the integrals with retarded propagators.

4.1 Amplitude computation

We start by calculating the LO three-body momentum-space amplitude $\mathcal{M}_s^{3,g}(1, 2, 3)$. The diagrams that contribute are shown in fig. 4. We generate them with **qgraf** [172], including all their symmetrizations and symmetry factors. The vertex Feynman rules were computed from eq. (3.1) with the help of **xAct** [173, 174]. We import the **qgraf**-diagrams, plug in Feynman rules and perform summation over indices with the help of **alibrary** [175]. Finally, we replace all scalar products with the minimal set of variables introduced in section 2.

In the next step, we generate the two-body NLO integrand from the generating three-body amplitude $\mathcal{M}_s^{3,g}(1, 2, 3)$. For that, we must set the background data of two black holes

to the same initial condition, thus identifying them with each other. In this way we obtain $\mathcal{M}_s^3(1, 2, 2)$ and $\mathcal{M}_s^3(1, 1, 2)$.

Next, we want to map the momenta in such a way, that the emerging integrals are mapped to the pentagon integral family (3.55) shown in fig. 7a. For simplicity we focus on the amplitude $\mathcal{M}_s^3(1, 2, 2)$ with mass scaling $m_1 m_2^2$. At a diagrammatic level we identify

$$\{m_3, v_3, b_3, \mathcal{S}_3\} \rightarrow \{m_2, v_2, b_2, \mathcal{S}_2\} , \quad (4.1)$$

to find all diagrams and thus the contributing Feynman amplitudes.

In order to map all integrals to the pentagon family (3.55) we use the linear map (3.51) for q_2 and q_3 . It turns out that two particular choices suffice to bring all diagrams of fig. 4 (and their symmetrizations) to the desired form:

$$L_1 : \quad q_2 \rightarrow \ell , \quad q_3 \rightarrow q_2 - \ell ; \quad (4.2)$$

$$L_2 : \quad q_2 \rightarrow q_2 - \ell , \quad q_3 \rightarrow \ell . \quad (4.3)$$

To make this clear, we next discuss an example diagram for each of the two mappings. Map L_1 is suitable for diagram 4b after the relabeling $(1, 2, 3) \rightarrow (1, 2, 2)$ of worldline data. The relabeled diagrams are shown in fig. 8a. For an application of map L_2 , we also consider diagram 4b, but for the label permutation $(1, 2, 3) \rightarrow (2, 1, 2)$. By comparing the propagator momenta of fig. 8b, it is clear that they match the ones of the pentagon family (3.55). The

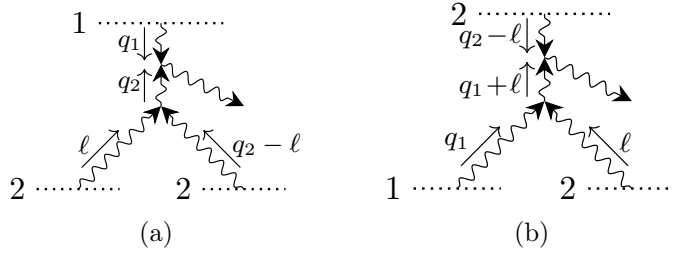


Figure 8: Example diagrams after momentum maps L_1 and L_2 were applied to relate their momenta to the ones of the pentagon family.

remaining diagrams follow in a similar way.

Technically, it is convenient to perform the momentum maps at the level of invariants. Considering eq. (2.7) we find that 9 out of the 14 variables map directly to the 5 variables of eq. (2.6). Those are

$$\begin{aligned} \omega_1 , \quad \omega_2 , \quad \omega_{31} \rightarrow \omega_2 , \quad \omega_3 \rightarrow \omega_2 , \quad q_1^2 , \quad q_{23}^2 \rightarrow q_2^2 , \\ y_{12} \rightarrow y , \quad y_{23} \rightarrow 1 , \quad y_{13} \rightarrow y . \end{aligned} \quad (4.4)$$

The remaining variables of the three-body scattering process can be written in terms of the external invariants or propagators of the two-body amplitude. This map then depends on

the specific maps (L_1 or L_2). The respective replacement rules are

$$L_1 : \quad \omega_{12} \rightarrow \rho_2 , \quad \omega_{23} \rightarrow -\rho_5 , \quad q_2^2 \rightarrow \rho_1 , \quad q_3^2 \rightarrow \rho_4 , \\ q_{12}^2 \rightarrow \rho_3 ; \quad (4.5)$$

$$L_2 : \quad \omega_{12} \rightarrow \omega_1 - \rho_1 , \quad \omega_{23} \rightarrow \rho_5 , \quad q_2^2 \rightarrow \rho_4 , \quad q_3^2 \rightarrow \rho_1 , \\ q_{12}^2 \rightarrow q_1^2 - q_2^2 + \rho_1 - \rho_3 + \rho_4 . \quad (4.6)$$

Performing these replacements on the diagrams of the three-body amplitude yields the integrand of the two-body momentum-space amplitude $\mathcal{M}_s^3(1, 2, 2)$ in terms of invariants and propagators. To simplify the expressions after the mapping to these loop integrands, we exploit diagram isomorphisms under transformations of ℓ and collect matching diagrams. Finally, the resulting tensor integrals were reduced to scalar integrals with the help of IBP relations using LITERED [176, 177]. The amplitude $\mathcal{M}_s^3(1, 1, 2)$ is obtained by relabeling.

4.2 Integrals

As a next step in the waveform computation, we must calculate the integrals in eq. (3.55). In particular, we have to consider all scalar master integrals $\mathcal{I}_{\vec{\nu}}$ with indices $\nu_i = 0, 1$. As above we focus on the integral family of $M_s^3(1, 2, 2)$ and obtain the integrals of $M_s^3(1, 1, 2)$ by relabeling.

So far, we have neglected to discuss the $i\epsilon$ prescription of the propagators. This aspect is the main focus of this section. For each propagator of the diagrams in fig. 4, the arrow shows a flow of causality towards the outgoing gravitational wave, which in turn specifies the retarded propagator prescriptions (3.26) and (3.27). As we discuss next, we find that, after integral reduction, these worldline integrals map onto the known field-theory Feynman integrals for the NLO waveform [146, 147, 150, 157].

The building block of the field-theory integrals is the Feynman integral

$$\widehat{\mathcal{I}}_{\vec{\nu}} = \int \frac{d^d \ell}{(2\pi)^d} \frac{1}{d_1^{\nu_1} d_2^{\nu_2} d_3^{\nu_3} d_4^{\nu_4} d_5^{\nu_5}} , \quad (4.7)$$

where

$$d_1 = \ell^2 + i\epsilon , \quad d_2 = v_1 \cdot \ell + i\epsilon , \quad d_3 = (\ell + q_1)^2 + i\epsilon , \\ d_4 = (\ell - q_2)^2 + i\epsilon , \quad d_5 = -v_2 \cdot \ell + i\epsilon . \quad (4.8)$$

and we assume $\nu_i = 0, 1$ below. Note that these propagators are equivalent to the WQFT ones (3.55) up to the $i\epsilon$ prescription. The integrals $\widehat{\mathcal{I}}$ are used to define the waveform master integrals $\widehat{\mathcal{I}}_{\vec{\nu}}^{\sigma_1, \sigma_2}$ [157] as the superposition

$$\widehat{\mathcal{I}}_{\vec{\nu}}^{\sigma_1, \sigma_2} \equiv \widehat{\mathcal{I}}_{\vec{\nu}} + (-1)^{\nu_2} \sigma_1 \widehat{\mathcal{I}}_{\vec{\nu}}|_{v_1 \rightarrow -v_1} + (-1)^{\nu_5} \sigma_2 \widehat{\mathcal{I}}_{\vec{\nu}}|_{v_2 \rightarrow -v_2} \\ + (-1)^{(\nu_2 + \nu_5)} \sigma_1 \sigma_2 \left(\widehat{\mathcal{I}}_{\vec{\nu}} - \text{Cut}_{d_2, d_5}[\widehat{\mathcal{I}}_{\vec{\nu}}] \right) |_{(v_1, v_2) \rightarrow (-v_1, -v_2)} , \quad (4.9)$$

where the cut-contribution is non-vanishing only for $\nu_2 = \nu_5 = 1$, and defined by

$$\text{Cut}_{d_2, d_5}[\widehat{\mathcal{I}}_{\vec{\nu}}] = \int \frac{d^d \ell}{(2\pi)^d} \frac{1}{d_1^{\nu_1} d_3^{\nu_3} d_4^{\nu_4}} [2\pi i \delta(d_2)] [2\pi i \delta(d_5)] . \quad (4.10)$$

We now show how the WQFT integrals \mathcal{I} of eq. (3.55) are equivalent to the integrals $\widehat{\mathcal{I}}_{\vec{\nu}}^{+-}$ and $\widehat{\mathcal{I}}_{\vec{\nu}}^{-+}$. We start with discussing the (in)sensitivity of the graviton propagators on their $i\epsilon$ -prescription and, in a second step, we show that the linear-propagator dependence matches.

Graviton propagators: The graviton propagators of the pentagon integral family (3.55) are d_1 , d_3 and d_4 , as defined in eq. (3.56). For those, the field-theory integrals $\widehat{\mathcal{I}}$ use the Feynman prescription (4.8), while the WQFT sets retarded propagators. Nevertheless, for the relevant parent topology, and hence for all its daughters, those two prescriptions give identical results.

To demonstrate this, we carefully study the momentum-conservation conditions

$$\delta(v_2 \cdot \ell) \delta(v_2 \cdot q_2) \delta(v_1 \cdot q_1) \delta^{(d)}(k - q_1 - q_2) , \quad (4.11)$$

of the diagram shown in fig. 7a, as generated by the Feynman rules. Furthermore we use that the energy of the produced gravitational wave is positive,

$$k^0 \geq 0 . \quad (4.12)$$

First, we recall that the $i\epsilon$ -prescription of the retarded graviton propagators $\{\rho_1, \rho_3, \rho_4\}$ depends on the sign of the energy component flowing in direction of causality. We now make the convenient frame choice, where $v_2 = (1, 0, 0, 0)$. The delta functions enforce vanishing energy components

$$v_2 \cdot \ell = \ell^0 = 0 \quad \text{and} \quad v_2 \cdot (\ell - q_2) = (\ell - q_2)^0 = 0 \quad (4.13)$$

for the propagators $\{\rho_1, \rho_4\}$, which are adjacent to worldline 2. In the cases where the energy component is 0, the $i\epsilon$ -dependence of the retarded propagator drops out completely, but that is not an issue. In such a case, the only possible divergent phase-space point must have vanishing momentum. Such a zero-dimensional singularity is integrable in $4 - 2\epsilon$ dimensions and the integrals do not require this contour deformation. Adding any $i\epsilon$ -prescription to the propagator will thus not change the result of the evaluated integral and we may choose the Feynman- $i\epsilon$ prescription. Next, we turn our attention to the graviton propagator ρ_3 . The respective graviton energy is positive,

$$(\ell + q_1)^0 = (\ell - q_2 + k)^0 = k^0 \geq 0 . \quad (4.14)$$

We may thus replace this retarded propagator by the appropriate Feynman propagator

$$\frac{1}{\rho_3} = \frac{1}{(\ell + q_1)^2 + i\epsilon \operatorname{sgn}(\ell^0 + q_1^0)} \rightarrow \frac{1}{d_3} = \frac{1}{(\ell + q_1)^2 + i\epsilon} . \quad (4.15)$$

Putting these observations together we can use the Feynman- $i\epsilon$ prescriptions for all graviton propagators in the integral family $\mathcal{I}_{\vec{\nu}}$,

$$\{\rho_1, \rho_3, \rho_4\} \rightarrow \{d_1, d_3, d_4\} . \quad (4.16)$$

Finally, we observe that we can use a uniform $i\epsilon$ -prescription for all graviton propagators of $\mathcal{I}_\nu^{\pm\mp}$. The only source of a mixed $i\epsilon$ -prescription is $1/d_1^*$ of the cut contribution (4.10). However, the delta functions of the cut integral (4.10) imply, like above, that the momentum of d_1 is space-like. Consequently, the respective propagator pole has vanishing support, and the $i\epsilon$ -prescription of $1/d_1^*$ is irrelevant. In this way we are allowed to replace

$$d_1^* \rightarrow d_1, \quad (4.17)$$

such that we may use Feynman propagators for all gravitons in $\widehat{\mathcal{I}}$.

Linear propagators: Having determined that the retarded graviton propagators can simply be replaced by Feynman propagators, we can factor them out of the sum (4.9). We next turn our attention to the matter propagators d_2 and d_5 , and show that they in fact match the ones of \mathcal{I} . For simplicity, we focus on the indices $\nu_2 = \nu_5 = 1$. (The reasoning simplifies for lower values of the indices $\nu_{2,5}$.) The matter propagators transform under the sign change of the velocities as

$$d_2 \xrightarrow{v_1 \rightarrow -v_1} -d_2^*, \quad d_5 \xrightarrow{v_2 \rightarrow -v_2} -d_5^*, \quad (4.18)$$

such that the field-theory integrals $\widehat{\mathcal{I}}$ turn into

$$\begin{aligned} \widehat{\mathcal{I}}_{\nu}^{\sigma_1, \sigma_2} &= \int \frac{d^d \ell}{(2\pi)^d} \frac{1}{d_1^{\nu_1} d_3^{\nu_3} d_4^{\nu_4}} \left(\frac{1}{d_2 d_5} + \frac{\sigma_1}{d_2^* d_5} + \frac{\sigma_2}{d_2 d_5^*} + \sigma_1 \sigma_2 \left[\frac{1}{d_2^* d_5^*} - \left(\frac{1}{d_2^*} - \frac{1}{d_2} \right) \left(\frac{1}{d_5^*} - \frac{1}{d_5} \right) \right] \right) \\ &= \int \frac{d^d \ell}{(2\pi)^d} \frac{1}{\rho_1^{\nu_1} \rho_3^{\nu_3} \rho_4^{\nu_4}} \left(\frac{1 - \sigma_1 \sigma_2}{d_2 d_5} + \frac{\sigma_1(\sigma_2 + 1)}{d_2^* d_5} + \frac{\sigma_2(\sigma_1 + 1)}{d_2 d_5^*} \right). \end{aligned} \quad (4.19)$$

Here we used eq. (3.54) to express delta functions in terms of propagators. Inserting $\sigma_1 = -\sigma_2 = 1$ we find,

$$\widehat{\mathcal{I}}_{\nu}^{+-} = -2 \int \frac{d^d \ell}{(2\pi)^d} \frac{1}{d_1^{\nu_1} d_2 d_3^{\nu_3} d_4^{\nu_4}} [2\pi i \delta(d_5)]. \quad (4.20)$$

Given that $\rho_2 = d_2$, the invariance (4.16) and the fact that the delta function $\delta(d_5)$ is insensitive to the $i\epsilon$ -prescription, this integral is proportional to the scalar integral $\widehat{\mathcal{I}}_{\nu}$ (3.55). Integrals belonging to the family with mass scaling $m_1^2 m_2$ can be found from exchanging $(1 \leftrightarrow 2)$ (or equivalently $\sigma_1 = -\sigma_2 = -1$).

We have thus shown that the WQFT computation requires the same integrals as the waveform calculation in field theory. A complete list of the required integrals was provided in ref. [157] (see also [150]).

5 Spinning waveforms from QFT amplitudes

In WQFT, the classical observables are directly captured by tree-level matrix elements. Alternatively, we can obtain the same observables from scattering amplitudes computed in a field theory of gravity and massive matter by taking a classical limit [151–153]. (This equivalence of WQFT and field-theory is expected on general grounds [178].) In the past,

we exploited the field-theory approach already for computing the linear-in-spin corrections to the waveform at NLO in the PM expansion [150]. Here, we will utilize this approach to cross check the generating WQFT amplitudes which make up the NLO WQFT integrand. Interpreted differently, we demonstrate a direct way to obtain classical integrands from field theory. We remark that hyper-classical terms do not appear in this construction.

For this purpose we employ the following field theory to capture the classical scattering

$$S = S_{\text{EH}} + S_{\text{gf}} + \sum_{i=1}^3 S_{(\phi_i, m_i)} + \sum_{i=1}^3 S_{(V_i, m_i)} , \quad (5.1)$$

with

$$S_{(\phi, m)} = \frac{1}{2} \int d^4x \sqrt{|g|} [g^{\mu\nu} (\partial_\mu \phi) (\partial_\nu \phi) - m^2 \phi^2] , \quad (5.2)$$

$$S_{(V, m)} = -\frac{1}{4} \int d^4x \sqrt{|g|} [g^{\mu\nu} g^{\alpha\beta} F_{\mu\alpha} F_{\nu\beta} - 2m^2 g^{\mu\nu} V_\mu V_\nu] , \quad (5.3)$$

where $F_{\mu\nu} = \partial_\mu V_\nu - \partial_\nu V_\mu$. In this theory we study the following scattering processes

$$\begin{aligned} \text{i : } & \phi_1(p_1) + \phi_2(p_2) + \phi_3(p_3) \rightarrow \phi_1(p'_1) + \phi_2(p'_2) + \phi_3(p'_3) + h(k^s) , \\ \text{ii : } & V_1(p_1^{s_1}) + \phi_2(p_2) + \phi_3(p_3) \rightarrow V_1(p_1'^{s'_1}) + \phi_2(p'_2) + \phi_3(p'_3) + h(k^s) , \\ \text{iii : } & V_1(p_1^{s_1}) + V_2(p_2^{s_2}) + \phi_3(p_3) \rightarrow V_1(p_1'^{s'_1}) + V_2(p_2'^{s'_2}) + \phi_3(p'_3) + h(k^s) , \end{aligned} \quad (5.4)$$

where the superscripts s, s_i and s'_i denote the spin quantum numbers. These scattering amplitudes allow us to capture up to quadratic-in-spin contributions [179] to the scattering of three spinning black holes. To recover the spin of black hole 3, we can permute labels in eq. (5.4). Furthermore, we parameterize the kinematic of these processes via

$$\begin{aligned} p_1 &= \bar{m}_1 v_1 + \frac{q_1}{2} , & p'_1 &= \bar{m}_1 v_1 - \frac{q_1}{2} , & p_2 &= \bar{m}_2 v_2 + \frac{q_2}{2} , & p'_2 &= \bar{m}_2 v_2 - \frac{q_2}{2} , \\ p_3 &= \bar{m}_3 v_3 + \frac{q_3}{2} , & p'_3 &= \bar{m}_3 v_3 - \frac{q_3}{2} , & k &= q_1 + q_2 + q_3 . \end{aligned} \quad (5.5)$$

The LO scattering amplitude, which we aim to relate to the generating amplitude $\mathcal{M}_s^{n,g}$ (3.40), is defined by

$$\begin{aligned} \langle p_1'^{s'_1}, \dots, p_n'^{s'_n}, k^s | T | p_1, \dots, p_n \rangle \Big|_{\text{tree diagrams}} = \\ (2\pi)^d \delta^d [p_1 + \dots + p_n - (k + p'_1 + \dots + p'_n)] M_{\vec{s}}^{\text{tree}, n} \end{aligned} \quad (5.6)$$

for the T -matrix convention $S = 1 + iT$ and $\vec{s} = \{s, s_1, s'_1, \dots, s_n, s'_n\}$. The tree-level amplitude $M_{\vec{s}}^{\text{tree}, n}$ depends linearly on the polarization states, and in particular $M_{\vec{s}}^{\text{tree}, 7}$ on the choices in eq. (5.4).

The most subtle piece of the computation is recovering a classical spin dependence from the amplitude $M_{\vec{s}}^{\text{tree}, n}$ written in terms of spin-1 polarization vectors. We use the Pauli-Lubanski operator (see e.g. [180]) given as

$$\mathbb{S}_\mu = \frac{1}{2m} \varepsilon_{\mu\nu\alpha\beta} p^\nu \mathbb{M}^{\alpha\beta} , \quad (5.7)$$

where $\mathbb{M}^{\rho\sigma}$ are the Lorentz-group generators. It is equal to the relativistic spin operator for a state with momentum p and mass m ($p^2 = m^2$). Two of the amplitudes $M_s^{\text{tree},7}$ for the processes listed in eq. (5.4) will depend on spin-1 polarization vectors $\varepsilon_v^\mu(p_i)$. To express those in terms of the Pauli-Lubanski operator we use a Clebsch-Gordan decomposition of a product of polarization states [181],

$$\begin{aligned} \bar{\varepsilon}_{v'}^\mu(p) \varepsilon_v^\nu(p) = & \frac{1}{3} \bar{\varepsilon}_{v'}(p) \cdot \mathbb{P} \cdot \varepsilon_v(p) \left(\eta^{\mu\nu} - \frac{p^\mu p^\nu}{m^2} \right) - \frac{i}{2m} \varepsilon^{\mu\nu\rho\sigma} p_\rho \bar{\varepsilon}_{v'}(p) \cdot \mathbb{S}_\sigma \cdot \varepsilon_v(p) \\ & + \bar{\varepsilon}_{v'}(p) \cdot \mathbb{S}^{\{\mu} \mathbb{S}^{\nu\}} \cdot \varepsilon_v(p), \end{aligned} \quad (5.8)$$

where we defined

$$\mathbb{S}^{\{\mu} \mathbb{S}^{\nu\}} \equiv \frac{1}{2} (\mathbb{S}^\mu \mathbb{S}^\nu + \mathbb{S}^\nu \mathbb{S}^\mu) - \frac{1}{3} (\mathbb{S} \cdot \mathbb{S}) \mathbb{P}^{\mu\nu}, \quad (5.9)$$

and

$$\mathbb{P}^{\mu\nu} \equiv \eta^{\mu\nu} - \frac{p^\mu p^\nu}{m^2}. \quad (5.10)$$

This decomposition can be obtained for polarization vectors which are defined for the same momentum. However, the amplitudes $M_s^{\text{tree},7}$ depend on polarization vectors given by incoming and outgoing momenta. Those polarization states differ by a Lorentz transformation. A boost that relates two generic momenta p and p' , which both belong to the same mass shell, is given by

$$\begin{aligned} \Lambda_\nu^\mu(p', p) = & \delta_\nu^\mu \\ & + \frac{1}{(p - p')^2 - 4m^2} \left[2 \frac{(p - p')^2}{m^2} p'^\mu p_\nu + 4(p - p')^\mu p_\nu - 2(p + p')^\mu (p - p')_\nu \right], \end{aligned} \quad (5.11)$$

where the two momenta p and p' fulfill $p^2 = p'^2 = m^2$. While the scalar contribution and linear-in-spin correction are insensitive to the frame choice, we must boost to the "central" frames related to \bar{p}_i to recover the correct quadratic-in-spin dependence [113]. Since $p_i^2 \neq \bar{p}_i^2$, we cannot relate the momenta directly by a Lorentz boost and we define

$$\bar{p}'_i = \frac{m_i}{\bar{m}_i} \bar{p}_i. \quad (5.12)$$

The classical spin dependence of the amplitude is therefore obtained by the replacement

$$\frac{\bar{\varepsilon}_v(\bar{p}'_i) \cdot \mathbb{S}^\mu \cdot \varepsilon_v(\bar{p}'_i)}{\bar{\varepsilon}_v(\bar{p}'_i) \cdot \varepsilon_v(\bar{p}'_i)} \rightarrow \mathcal{S}_i^\mu \quad \text{and} \quad M_s^{\text{tree},7} \rightarrow M_s^{\text{tree},7}(\mathcal{S}), \quad (5.13)$$

after relating the polarization states of the momenta \bar{p}'_i and p_i by a boost.

To extract the classical information and remove any quantum corrections, we take the classical point-mass limit via $\bar{m}_i \rightarrow \infty$, which we implement through scaling $\bar{m}_i \rightarrow x \bar{m}'_i$ and performing a series expansion around infinite x ,

$$x \rightarrow \infty \quad \text{with} \quad \left\{ \bar{m}'_i, y_{ij}, q_{ij}^2, q_{ij}^2, \omega_i, \omega_{ij}, \frac{\mathcal{S}_i}{x}, \sqrt{x} \kappa \right\} = \text{fixed}. \quad (5.14)$$

The seven-point tree-level amplitudes $M_s^{\text{tree},7}$ scale as

$$M_s^{\text{tree},7}(\mathcal{S}) \sim \kappa^5 x^5 (\mathcal{S}/x)^{n_S} + \text{sub-leading terms}, \quad (5.15)$$

where $n_{\mathcal{S}}$ is the order of the spin multipole contribution. The classical amplitude is identified as the leading term in the scaling limit,

$$\mathcal{M}_s^{\text{tree},7}(\mathcal{S}) = M_s^{\text{tree},7}(\mathcal{S}) \Big|_{\text{leading x-scaling}}. \quad (5.16)$$

The classical field theory amplitude is expected to match the WQFT momentum-space amplitude

$$\mathcal{M}_s^{3,g} = \frac{1}{8 m_1 m_2 m_3} \mathcal{M}_s^{\text{tree},7}(\mathcal{S}), \quad (5.17)$$

which we confirm. The relative factor between the amplitudes in eq. (5.17) is compensated by the phase-space measure of the KMOC formalism, such that the impact-parameter waveforms match identically. We would like to emphasise that $M_s^{\text{tree},n}$ is a field theory tree-level amplitude, which allows to construct the waveform integrand. It matches the WQFT generating amplitudes and is free of hyper-classical contributions. Furthermore, the construction generalizes to higher multiplicity and, after source identification, to higher order corrections.

An extra subtlety in this approach is obtaining the Casimir corrections ($\sim \mathcal{S}^2$). The issue arises because at the level of operators, we may make the replacement $\mathcal{S}^2 \rightarrow -s(s+1)\mathbb{1}$, which moves terms of the quadratic-in-spin correction to quantum corrections of the scalar contribution, and is known as the *Casimir ambiguity*. We employ the *spin interpolation* method [113], to extract the spin Casimir contributions by interpolating between spinless and spinning amplitudes. In more detail, working in a $s = 1$ theory, we add a term $\frac{c}{x^2}(\mathcal{S}^2 + 2)$ with an undetermined coefficient c . We take advantage of *spin universality* to fix said coefficient; by comparing to a calculation done in an $s = 0$ theory, we require the leading-order and first quantum correction to be equivalent to the scalar contribution obtained in the $s = 1$ calculation, which uniquely determines the coefficient c , and thus also fixes the Casimir contribution.

Implementation: For the comparison with the WQFT seven-point tree-level amplitudes, a numerical result of the classical field-theory amplitude is sufficient. We perform the numerical computation of the field-theory amplitudes $M_{\vec{s}}^{\text{tree},n}$ (5.6) within the CARAVEL framework [156]. This requires a tensor decomposition where the dependence on the polarization vectors (or spin) is captured by a basis of rank-two tensors, and the coefficients (called form-factors) can be calculated numerically. We use the same auxiliary tensor basis $\{T_1^{\alpha\beta}, \dots, T_9^{\alpha\beta}\}$ as defined in ref. [150]. Those we contract with the polarization vectors for $i = 1, 2$ defined through boost from the \vec{p}'_i frame

$$T_{n,i}^{v'v} = \bar{\varepsilon}_{v'}(p'_i) \cdot T_n \cdot \varepsilon_v(p_i) = \bar{\varepsilon}_{v'}(\vec{p}'_i) \cdot [\Lambda(\vec{p}'_i, p'_i) \cdot T_n \cdot \Lambda(p_i, \vec{p}_i)] \cdot \varepsilon_v(\vec{p}_i). \quad (5.18)$$

We relate them to the classical spin and define

$$T_{n,i}^{\text{cl}}(\mathcal{S}) = -[\Lambda(\vec{p}'_i, p'_i) \cdot T_{n,i} \cdot \Lambda(p_i, \vec{p}_i)]_{\mu\nu} \left[\frac{1}{3} \left(\eta^{\mu\nu} - \frac{\vec{p}_i^\mu \vec{p}_i^\nu}{m_i^2} \right) - \frac{i}{2m_i} \epsilon^{\mu\nu\rho\sigma} \vec{p}'_{i\rho} \mathcal{S}_{i\sigma} + \mathcal{S}_i^{\{\mu} \mathcal{S}_i^{\nu\}} \right]. \quad (5.19)$$

Finally, we reconstruct the analytic dependence on x from multiple numerical evaluations, which allows us to take the classical limit $x \rightarrow \infty$. The so obtained classical scattering amplitude can be directly compared to the three-body amplitude computed within the WQFT formalism.

6 Results

In this section, we collect the classical momentum-space waveform, excluding the (not detectable) static background contribution, up to $\mathcal{O}(G^3\mathcal{S}^2)$. We split the discussion into the three-body waveform and the two-body waveform. We further discuss the regularization of its divergences and other analytic properties.

6.1 Leading-order three-body momentum-space waveform

As explained in detail in section 4, we compute as a side product the leading-order waveform for the scattering of three spinning black holes including quadratic spin terms,

$$\mathcal{M}_s^{3,\text{LO}} = \mathcal{M}_s^3(1, 2, 3). \quad (6.1)$$

The waveform is obtained from $3 \rightarrow 4$ tree-level amplitudes and has the following multipole expansion

$$\mathcal{M}_s^{3,\text{LO}} = t_0 + \sum_{i=1}^3 t_{\mu\nu}^{(i)} \mathcal{S}_i^{\mu\nu} + \sum_{i,j=1}^3 t_{\mu\nu\rho\sigma}^{(ij)} \mathcal{S}_i^{\mu\nu} \mathcal{S}_j^{\rho\sigma} \quad (6.2)$$

in terms of the anti-symmetric coefficients $t_{\mu\nu}^{(i)} = t_{[\mu\nu]}^{(i)}$ and $t_{\mu\nu\rho\sigma}^{(ij)} = t_{[\mu\nu][\rho\sigma]}^{(ij)}$. We are providing the analytic results for these multipole coefficients in the ancillary files of this article. We would like to emphasize the fact that the result is expressed in terms of 14 kinematic invariants, see section 2, which are linear independent for general d -dimensional external kinematics. The number of kinematic variables can be further reduced for strictly four-dimensional momenta using Gram-determinant relations and might lead to more compact expressions.

6.2 Next-to-leading order two-body momentum-space waveform

For the scattering of two black holes, we give the waveform up to NLO in G and quadratic in spin, i.e at $\mathcal{O}(G^3\mathcal{S}^2)$. This captures several spin-interaction effects of the scattering. At linear order in spin, we obtain the spin-orbit coupling $v_i \cdot \mathcal{S}_j$, while at quadratic order in spin, we additionally capture the spin-spin couplings $\mathcal{S}_1 \cdot \mathcal{S}_2$, and the first self-interaction spin contributions \mathcal{S}_i^2 .

To exclude the static background, we define the momentum space LO and NLO binary waveform through

$$\mathcal{M}_s^{2,\text{LO}} = \mathcal{M}_{\text{tree}} = \mathcal{M}_s^2(1, 2), \quad (6.3)$$

$$\mathcal{M}_s^{2,\text{NLO}} = \mathcal{M}_s^2(1, 2) + \mathcal{M}_s^3(1, 1, 2) + \mathcal{M}_s^3(1, 2, 2), \quad (6.4)$$

where we introduced the redundant notation $\mathcal{M}_{\text{tree}}$ for convenience and consistency with ref. [150]. We split the amplitude into its tree-level contribution, an infrared (IR) divergent piece, an ultraviolet (UV) divergent piece, a scale dependent tail contribution and a finite contribution. The waveform thus reads

$$\mathcal{M}_s^{2,\text{NLO}} = \mathcal{M}_{\text{tree}} + \mathcal{M}_{\text{IR}} + \mathcal{M}_{\text{UV}} + \mathcal{M}_{\text{tail}} + \mathcal{M}_{\text{finite}}. \quad (6.5)$$

Next, we briefly discuss each contribution to the NLO waveform.

Leading-order waveform: The leading-order piece of the two-body waveform up to \mathcal{S}^2 was first calculated in refs. [142] (later confirmed by refs. [143–145]) and we find an equivalent expression. The five-point tree amplitude contains terms suppressed by the dimensional regulator ϵ . While not relevant at leading order, we keep it in the IR subtraction at higher order. We split the tree as

$$\mathcal{M}_{\text{tree}} = \mathcal{M}_{\text{tree}}^{\epsilon^0} + \epsilon \mathcal{M}_{\text{tree}}^{\epsilon^1} + \mathcal{O}(\epsilon^2). \quad (6.6)$$

where the higher-order terms in ϵ arise working in the 't Hooft-Veltman scheme. Namely, we performed the Lorentz algebra in d dimensions, while keeping the external states in four dimensions. The term $\mathcal{M}_{\text{tree}}^{\epsilon^1}$ becomes relevant in our definition of the NLO waveform.

Infrared divergence: As in the scattering-amplitude approach, the gravitational waveform develops IR divergences. The IR divergences factorize and their contribution takes the form

$$\mathcal{M}_{\text{IR}} = \left[\frac{1}{\epsilon} - \log \left(\frac{\mu_{\text{IR}}^2}{\mu^2} \right) \right] \mathcal{W}_S \mathcal{M}_{\text{tree}}, \quad (6.7)$$

where \mathcal{W}_S is the soft factor of the waveform [147, 150, 182] and is given by

$$\mathcal{W}_S = -iG(m_1\omega_1 + m_2\omega_2) \left[1 + \frac{y(2y^2 - 3)}{2(y^2 - 1)^{3/2}} \right]. \quad (6.8)$$

As expected, the IR divergence scales with the tree. Because of this, we can exponentiate it. To obtain a finite waveform, we may absorb this IR divergence into a phase [51, 110, 146, 183]. The waveform in time domain is computed through a Fourier transformation from frequency domain to time domain, given in eq. (3.18). This Fourier transformation includes a phase depending on the retarded-time variable, which is used to absorb the IR divergence:

$$e^{-i\omega(t-|\mathbf{r}|)} \mathcal{M}_s^{2,\text{NLO}} = e^{-i\omega \left[t-|\mathbf{r}| + \left(\frac{1}{\epsilon} - \log \frac{\mu_{\text{IR}}^2}{\mu^2} \right) \frac{\mathcal{W}_S}{i\omega} \right]} \left(\mathcal{M}_{\text{tree}} + \mathcal{M}_{\text{UV}} + \mathcal{M}_{\text{tail}} + \mathcal{M}_{\text{finite}} \right) + \mathcal{O}(G^3). \quad (6.9)$$

Note that we have absorbed a term $\mathcal{W}_S \mathcal{M}_{\text{tree}}^{\epsilon^1}$ into the finite terms after IR subtraction. This piece is related to a ϵ/ϵ contribution from the IR.

It is interesting to note that the redefinition of retarded time $t - |\mathbf{r}|$ may also be found from a general relativistic approach [150, 157]. It is related to the Shapiro delay of a graviton climbing out of a potential well to infinity [184] and the deflection of the incoming trajectory of the two scattering black holes due to the Kerr spacetime at infinity.

Ultraviolet divergences: As in the scattering amplitude approach [146–150], the two-body waveform develops an UV divergence in the WQFT as well. Its contribution takes the form

$$\mathcal{M}_{\text{UV}} = \left[\frac{1}{\epsilon} - \log \left(\frac{\mu_{\text{UV}}^2}{\mu^2} \right) \right] \bar{\mathcal{M}}_{\text{UV}}. \quad (6.10)$$

Here, $\bar{\mathcal{M}}_{\text{UV}}$ depends polynomially on the momentum exchanges q_1 and q_2 . After a Fourier transformation from momentum to impact parameter space, they will only yield contributions local in the impact parameter b (i.e. $\sim \delta(|b|)$). We may thus drop them when considering the far-field waveform.

Tail contribution: The tail contribution of the waveform amounts to

$$\mathcal{M}_{\text{tail}} = -\log \left(\frac{\omega_1 \omega_2}{\mu_{\text{IR}}^2} \right) \mathcal{W}_S \mathcal{M}_{\text{tree}} - \log \left(\frac{\omega_1 \omega_2}{\mu_{\text{UV}}^2} \right) \bar{\mathcal{M}}_{\text{UV}}. \quad (6.11)$$

While the UV pole including the factor $\bar{\mathcal{M}}_{\text{UV}}$ does not contribute to the far-field waveform, the tail has been found to dominate in the scattering waveform of two Schwarzschild black holes [146].

Finite contributions: At last, the finite remainder of the NLO waveform can be written as a linear combination of special functions f_i that span the linear independent functions of all necessary Feynman integrals. We can write the finite remainder as

$$\mathcal{M}_{\text{finite}} = \sum_{i=1}^{18} r_i f_i, \quad (6.12)$$

where the functions f_i can be found in the appendix of ref. [150] (after adjusting to the different convention by mapping $\omega_i \rightarrow -\omega_i$). We provide the coefficients r_i and the definition of the functions f_i in the ancillary files.

Ancillary files: We provide ancillary files containing the two-body and three-body waveform in momentum space up to $\mathcal{O}(G^3 \mathcal{S}^2)$. Their folder structure is:

`anc/waveform.m`

`anc/waveform3BH.m`

`anc/loadWaveform.wl`

The file `waveform.m` contains the different contributions to the two-body waveform up to quadratic order in spin. The spin dependence is given in terms of the spin tensors $\mathcal{S}_i^{\mu\nu}$ contracted with external momenta, other spin tensors or itself. The waveform has been contracted with a gravitational-wave polarization tensor $\varepsilon^{\mu\nu}(k) = \varepsilon^\mu(k) \varepsilon^\nu(k)$. The analytic expression for the three-body waveform can be found in the file `waveform3BH.m`. To access the waveform, the file `loadWaveform.wl` contains commands to load and use the results. It furthermore contains details on the notation.

6.3 BMS frame

By ignoring contributions due to zero-frequency modes of the gravitational wave ($\sim \delta(\omega)$), we have automatically chosen the *canonical* Bondi-Metzner-Sachs (BMS) frame [185–187]. The methods traditionally used to calculate gravitational waves emitted during the inspiral and merger of two black holes are on the other hand in the *intrinsic* BMS frame [154, 188]. The results in the two frames are related by a supertranslation and one can recover the waveform in the intrinsic frame from the waveform in the canonical frame by shifting the time t [188–190]

$$t \rightarrow t + 2G \left(m_1 v_1 \cdot \hat{k} \log(v_1 \cdot \hat{k}) + m_2 v_2 \cdot \hat{k} \log(v_2 \cdot \hat{k}) \right), \quad (6.13)$$

where $\hat{k} = k/\omega$. This shift also recovers the static background at $\mathcal{O}(G)$ [187].

6.4 Validation

We validate our results through analytic consistency checks and numerical comparisons at various stages of the computation. A discussion of the behavior of the waveform under supersymmetry transformations can be found in appendix B.

Gauge invariance: We explicitly verify the gauge invariance of both the three-body and two-body waveforms by confirming that

$$\lim_{k^2 \rightarrow 0} k^2 k_\mu h_{\text{cl}}^{\mu\nu}(k) = 0 \quad (6.14)$$

in both cases.

Three-body waveform: The scalar component of our three-body waveform reproduces the result of ref. [140]. In addition, we perform a numerical cross-check against the independent QFT computation including all spin-squared contributions, as discussed in section 5.

WQFT integrals: We validate the WQFT integrals against refs. [146, 147, 150, 157] and by numerically evaluating them using AMFlow [191] and find agreement with our analytic expressions.

Two-body waveform: For the two-body case, we benchmark the spinless NLO waveform against previous results [146–148, 150, 192], and confirm agreement. The linear-in-spin contribution is likewise consistent with ref. [150]. Furthermore, we verify that the IR divergence matches the expectation from Weinberg’s soft-graviton theorem, while the UV divergence does not contribute to the final observable waveform. Moreover, the two-body waveform is constructed from the previously validated three-body waveform. Finally, we verify that the NLO waveform is regular in phase space, by confirming that spurious poles in the function coefficients cancel.

7 Conclusion

In this work, we presented the quadratic-in-spin contributions to the gravitational waveform emitted during the scattering of two spinning black holes at next-to-leading PM order, i.e. at $\mathcal{O}(G^3\mathcal{S}^2)$. Our calculation is based on the WQFT formalism [120–123] that allows to compute classical observables directly from tree-level amplitudes in the Keldysh-Schwinger formalism [163, 164]. In particular, we closely follow the supersymmetric variant [142, 160] of the WQFT formalism to obtain classical spin effects. We have extensively reviewed the formalism and showed the expected consistency [178] between the WQFT and scattering-amplitude results. In our discussion, we placed particular emphasis on identifying generating WQFT amplitudes (see e.g. [120]), which resemble loop-amplitude integrands and may equivalently be obtained from tree-level amplitudes in field-theory [155]. Furthermore, we confirmed the applicability of the cut-improved Feynman integral basis [157] for the retarded radiation dynamic. As a by-product, we also obtained for the first time the LO gravitational waveform for the scattering of three spinning black holes.

To further highlight the similarities between the two approaches, we verified our WQFT results by comparing to scattering amplitudes of scalars, Proca fields and gravitons. The latter approach uses familiar Feynman rules and provides a sturdy cross-check, but obtaining classical observables through loop computations appeared to be less direct: hyper-classical terms appear and cancel only in the final result [146–150]. Furthermore, re-expressing polarization vectors in terms of classical spin—while keeping the correct Casimir contribution—can be subtle. Performing these steps numerically and reconstructing only the newly introduced generating amplitude proved useful. In this comparison we extracted the spin Casimir operator contributions by employing the spin-interpolation method [113, 117] which adds further evidence for its validity. Taken together, the WQFT offers a direct route to analytic expressions, while the scattering-amplitudes approach supplies a robust numerical validation, and we exploit the strengths of both frameworks throughout this work.

We performed several additional validation steps on our results, such as checking Ward identities, consistency with the known factorization of infrared divergences [182], and reproducing the known spin-independent [143–145, 150, 162] and linear-in-spin contributions to the NLO waveform [150]. Finally, we confirmed the expected regularity of the waveform in phase space.

One natural follow-up direction is to extend our current techniques by employing the recent higher-spin extension of the WQFT formalism [161] to obtain the gravitational waveform up to the quartic order in spin. To obtain the actual observable analytically, it remains to perform the Fourier transformation to impact-parameter space. This has turned out to be a highly non-trivial task [146, 150] and we expect further challenges in higher-spin contributions. However, we anticipate that the method of ref. [168] will simplify this step tremendously. Additionally, so far our results describe scattering of black holes. It would be interesting to make use of the analytic continuation of the waveform, as proposed in refs. [193, 194], to obtain a gravitational waveform also for bound binary systems of spinning black holes. Finally, our results can be used to obtain the angular momentum and radiation reaction at $\mathcal{O}(G^4)$ [195] for rotating black holes. We leave these open questions

for future investigation.

Acknowledgments

L.B. acknowledges support from the Swiss National Science Foundation (SNSF) under the grant 200020 192092. L.B. thanks the UZH Candoc Grant for financial support. M.K. is supported by the DGAPA-PAPIIT grant IA102224 (“Iluminando agujeros negros”) at UNAM.

A Feynman rules

In this appendix we provide the vertex Feynman rules extracted from the WQFT action (3.1). For graviton self-interactions we make use of the FEYNGRAV program [196] to compute the corresponding Feynman rules.

In the following we will often need to symmetrize in Lorentz indices, and we introduce the operator $P^{(\mu\nu)}$ which symmetrises tensors $t_{\mu\nu}$

$$P^{(\mu_1, \nu_1)}(t_{\mu_1 \nu_1}) = t_{(\mu_1 \nu_1)}, \quad (\text{A.1})$$

following the notation of eq. (3.10). For consecutive symmetrization we use the notation

$$P^{(\mu_1, \nu_1) \dots (\mu_n, \nu_n)} = P^{(\mu_1, \nu_1)} \dots P^{(\mu_n, \nu_n)}. \quad (\text{A.2})$$

One-graviton worldline vertex

$$\begin{array}{c} \text{.....} \\ | \\ \text{wavy line} \\ | \\ k \\ \downarrow \\ h_{\mu\nu} \end{array} = -i \frac{m\kappa}{2} e^{ik \cdot b} \hat{\delta}(k \cdot v) \left[v^{(\mu} v^{\nu)} + \frac{i}{m} (k \cdot \mathcal{S})^{(\mu} v^{\nu)} - \frac{1}{2m^2} (k \cdot \mathcal{S})^{(\mu} (k \cdot \mathcal{S})^{\nu)} \right] \quad (\text{A.3})$$

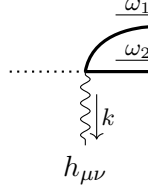
One-graviton one-scalar worldline vertex

$$\begin{array}{c} \text{.....} \xrightarrow{\omega} z^\rho \\ | \\ \text{wavy line} \\ | \\ k \\ \downarrow \\ h_{\mu\nu} \end{array} = \frac{m\kappa}{2} e^{ik \cdot b} \hat{\delta}(k \cdot v + \omega) \left(2\omega v^{(\mu} \delta_\rho^{\nu)} + v^{(\mu} v^{\nu)} k_\rho + \frac{i}{m} (k \cdot \mathcal{S})^{(\mu} (k_\rho v^{\nu)} + \omega \delta_\rho^{\nu)} \right) + \frac{1}{2m^2} (k \cdot \mathcal{S})^\mu (\mathcal{S} \cdot k)^\nu k_\rho \quad (\text{A.4})$$

One-graviton one-Grassmann-field vertex

$$\begin{array}{c} \text{.....} \xrightarrow{\omega} \phi^\sigma \\ | \\ \text{wavy line} \\ | \\ k \\ \downarrow \\ h_{\mu\nu} \end{array} = -im\kappa e^{ik \cdot b} \hat{\delta}(k \cdot v + \omega) \left(k_{[\sigma} \delta_{\xi]}^{(\mu} v^{\nu)} - \frac{i}{m} k_{[\sigma} \delta_{\xi]}^{(\mu} (\mathcal{S} \cdot k)^{\nu)} \right) \bar{\Psi}^\xi \quad (\text{A.5})$$

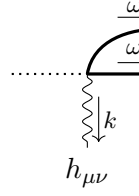
One-graviton two-scalar worldline vertex



$$z^{\rho_1} = m\kappa e^{ik \cdot b} \hat{\delta}(k \cdot v + \omega_1 + \omega_2) \times$$

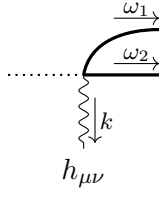
$$\left[i \left(\frac{1}{2} k_{\rho_1} k_{\rho_2} v^{(\mu} v^{\nu)} + \omega_1 k_{\rho_2} v^{(\mu} \delta_{\rho_1}^{\nu)} + \omega_2 k_{\rho_1} v^{(\mu} \delta_{\rho_2}^{\nu)} + \omega_1 \omega_2 \delta_{\rho_1}^{(\mu} \delta_{\rho_2}^{\nu)} \right) \right. \\ \left. + \frac{1}{2m} (\mathcal{S} \cdot k_{\sigma})^{(\mu} (\omega_1 k_{\rho_2} \delta_{\rho_1}^{\nu)} + \omega_2 k_{\rho_1} \delta_{\rho_2}^{\nu)} + k_{\rho_1} k_{\rho_2} v^{\nu)} \right. \\ \left. - \frac{1}{4m^2} i (\mathcal{S} \cdot k)^{(\mu} (\mathcal{S} \cdot k)^{\nu)} k_{\rho_1} k_{\rho_2} \right] \quad (\text{A.6})$$

One-graviton one-scalar one-Grassmann-field worldline vertex

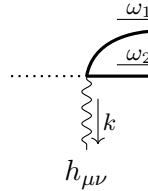


$$\phi^\sigma = -\frac{m\kappa}{2} e^{ik \cdot b} \hat{\delta}(k \cdot v + \omega_z + \omega_\phi) \left[\left(\delta_\sigma^{(\mu} (k \cdot \bar{\Psi}) - k_\sigma \bar{\Psi}^{(\mu)} \right) \right. \\ \left. \times \left(v^{\nu)} k_\rho + \omega_z \delta_\rho^\nu - \frac{i}{m} (\mathcal{S} \cdot k)^{\nu)} k_\rho \right) \right] \quad (\text{A.7})$$

One-graviton two-Grassmann-field worldline vertex

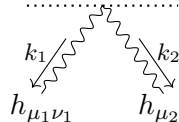


$$\bar{\phi}^\chi = im\kappa e^{ik \cdot b} \hat{\delta}(k \cdot v + \omega_1 + \omega_2) \left(\delta_{[\sigma}^{(\mu} k_{1, \chi]} v^{\nu)} - \frac{1}{2} \delta_\chi^{(\mu} \delta_\sigma^{\nu)} (k \cdot \Psi) (k \cdot \bar{\Psi}) \right. \\ \left. + \frac{1}{2} k_\chi \delta_\sigma^{(\mu} (k \cdot \Psi) \bar{\Psi}^{\nu)} - \frac{1}{2} k_\sigma \delta_\chi^{(\mu} (k \cdot \bar{\Psi}) \Psi^{\nu)} - \frac{1}{2} k_\sigma k_\chi \Psi^{(\mu} \bar{\Psi}^{\nu)} \right) \quad (\text{A.8})$$



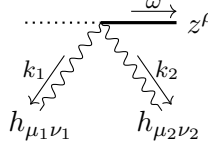
$$\phi^{\sigma_2} = im\kappa e^{ik \cdot b} \hat{\delta}(k \cdot v + \omega_1 + \omega_2) \delta_{[\sigma_1}^{(\mu} k_{\sigma_2]} \bar{\Psi}^{\nu)} (k \cdot \bar{\Psi}) \quad (\text{A.9})$$

Two-graviton worldline vertex



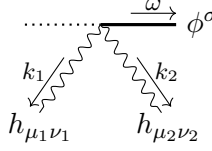
$$= P^{(\mu_1, \nu_1)(\mu_2, \nu_2)} \left[-\frac{\kappa^2}{4} e^{i(k_1 + k_2) \cdot b} \hat{\delta}((k_1 + k_2) \cdot v) \left((k_1 \cdot S)^{\mu_2} v^{\mu_1} \eta^{\nu_1 \nu_2} \right. \right. \\ \left. \left. - S^{\mu_1 \mu_2} (v^{\nu_1} k_1^{\nu_2} - \frac{1}{2} k_1 \cdot v \eta^{\nu_1 \nu_2}) + \frac{i}{m} \left[((S \cdot k_1)^{\mu_1} (S \cdot k)^{\mu_2} \right. \right. \right. \\ \left. \left. + \frac{1}{2} (S \cdot k_2)^{\mu_1} (S \cdot k_1)^{\mu_2} - \frac{1}{2} S^{\mu_1 \mu_2} (k_1 \cdot S \cdot k_2) \right) \eta^{\nu_1 \nu_2} \right. \right. \\ \left. \left. + \frac{1}{4} k_1 \cdot k_2 S^{\mu_1 \nu_2} S^{\mu_2 \nu_1} - k_1^{\nu_2} (S \cdot (k_1 + k_2)^{\mu_1}) S^{\mu_2 \nu_1} \right] \right) + (1 \leftrightarrow 2) \right] \quad (\text{A.10})$$

Two-graviton one-scalar worldline vertex



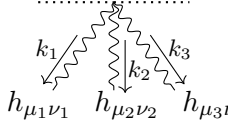
$$\begin{aligned}
&= P^{(\mu_1, \nu_1)(\mu_2, \nu_2)} \left[\frac{\kappa^2}{4} e^{i(k_1+k_2) \cdot b} \hat{\delta}((k_1+k_2) \cdot v + \omega) \left(i(k_1+k_2)_\rho [v^{\mu_1} k_1^{\mu_2} S^{\nu_1 \nu_2} \right. \right. \\
&\quad + \eta^{\mu_1 \mu_2} (S \cdot k_1)^{\nu_2} v^{\nu_1} - \frac{1}{2} \eta^{\mu_1 \mu_2} k_1 \cdot v S^{\nu_1 \nu_2}] + i\omega [\delta_\rho^{\mu_1} \eta^{\nu_1 \nu_2} (S \cdot k_1)^{\mu_2} \\
&\quad + \delta_\rho^{\mu_1} k_1^{\mu_2} S^{\nu_1 \nu_2} - \frac{1}{2} \eta^{\mu_1 \mu_2} k_{1\rho} S^{\nu_1 \nu_2}] \\
&\quad \left. \left. + \frac{1}{m} (k_1+k_2)_\rho [\eta^{\mu_1 \mu_2} (S \cdot k_1)^{\nu_2} + k_1^{\mu_2} S^{\mu_1 \nu_2}] (S \cdot k_1)^{\nu_1} \right) + (1 \leftrightarrow 2) \right] \quad (\text{A.11})
\end{aligned}$$

Two-graviton one-Grassmann-field worldline vertex



$$\begin{aligned}
&= P^{(\mu_1, \nu_1)(\mu_2, \nu_2)} \left[\frac{m\kappa^2}{4} e^{i(k_1+k_2) \cdot b} \hat{\delta}((k_1+k_2) \cdot v + \omega) \left(i[\eta^{\mu_1 \mu_2} k_{1\sigma} v^{\nu_1} \bar{\Psi}^{\nu_2} \right. \right. \\
&\quad + \delta_\sigma^{\mu_1} (k_2^{\nu_1} v^{\mu_2} - k_1^{\mu_2} v^{\nu_1} + \frac{1}{2} (k_1 - k_2) \cdot v \eta^{\mu_2 \nu_1}) \bar{\Psi}^{\nu_2} - \eta^{\mu_1 \mu_2} \delta_\sigma^{\nu_2} v^{\nu_1} k_1 \cdot \bar{\Psi}] \\
&\quad + \frac{1}{m} [\eta^{\mu_1 \mu_2} ((S \cdot k_1)^{\nu_1} k_{1\sigma} + (S \cdot k_2)^{\nu_1} k_{2\sigma}) \bar{\Psi}^{\nu_2} + \delta_\sigma^{\mu_1} ((S \cdot k_2)^{\mu_2} k_2^{\nu_1} \\
&\quad - (S \cdot k_1)^{\nu_1} k_1^{\mu_2}) \bar{\Psi}^{\nu_2} - \delta_\sigma^{\nu_1} k_1^{\nu_2} S^{\mu_1 \mu_2} k_1 \cdot \bar{\Psi} - \delta_\sigma^{\mu_1} \eta^{\nu_1 \mu_2} (k_1 \cdot \bar{\Psi} (S \cdot k_1)^{\nu_2} \\
&\quad + k_2 \cdot \bar{\Psi} (S \cdot k_2)^{\nu_2}) - k_{2\sigma} k_2^{\mu_1} S^{\nu_1 \mu_2} \bar{\Psi}^{\nu_2}] + (1 \leftrightarrow 2) \Big] \quad (\text{A.12})
\end{aligned}$$

Three-graviton worldline vertex



$$\begin{aligned}
&= P^{(\mu_1, \nu_1)(\mu_2, \nu_2)(\mu_3, \nu_3)} \left[\frac{\kappa^3}{8} e^{i(k_1+k_2+k_3) \cdot b} \hat{\delta}((k_1+k_2+k_3) \cdot v) \right. \\
&\quad \times \left(g^{\mu_2 \mu_3} \left[(g^{\mu_1 \nu_3} k_1 \cdot v + k_3^{\mu_1} v^{\nu_3}) S^{\nu_1 \nu_2} + \frac{3}{2} (k_1^{\nu_3} S^{\nu_2 \mu_1} - g^{\mu_1 \nu_3} (S \cdot k_1)^{\nu_2}) v^{\nu_1} \right] \right. \\
&\quad + \frac{i}{m} \left[g^{\mu_2 \mu_3} g^{\mu_1 \nu_3} (S \cdot (k_2 + \frac{3}{2} k_1))^{\nu_1} (S \cdot k_1)^{\nu_2} \right. \\
&\quad + \frac{1}{2} g^{\mu_1 \mu_2} g^{\mu_3 \nu_1} (S \cdot k_1)^{\nu_2} (S \cdot k_1)^{\nu_3} - g^{\mu_2 \mu_3} [(S \cdot k_2)^{\nu_3} k_2^{\mu_1} \\
&\quad - 2(S \cdot k_2)^{\mu_1} k_1^{\nu_3} + k_3^{\mu_1} (S \cdot k_3)^{\nu_3} + g^{\mu_1 \nu_3} k_1 \cdot S \cdot k_2] S^{\nu_1 \nu_2} \\
&\quad \left. \left. + \frac{1}{2} [k_2^{\mu_1} k_2^{\nu_3} S^{\mu_3 \mu_2} - k_1^{\nu_3} k_2^{\mu_3} S^{\mu_1 \mu_2} - 2g^{\mu_1 \mu_3} (S \cdot k_2)^{\mu_2} k_2^{\nu_3}] S^{\nu_1 \nu_2} \right] \right) \\
&\quad \left. + \text{permutations}(1, 2, 3) \right] \quad (\text{A.13})
\end{aligned}$$

B Worldline supersymmetry property

We confirm that the two-body and three-body integrand both are consistent with eq. (26) of ref. [142], that links higher-spin orders to lower-spin. These relations can be derived from the worldline-supersymmetry transformations and are naturally fulfilled when spin tensors

obey the covariant spin-supplementary condition (2.10). In fact, in the three-body case, the relations are

$$\frac{i}{2}q_{i\mu}t_0 = v_i^\nu t_{\mu\nu}^{(i)}, \quad \frac{i}{4}q_{j\rho}t_{\mu\nu}^{(i)} = v_j^\sigma t_{\mu\nu\rho\sigma}^{(ij)}, \quad (\text{B.1})$$

where the tensors t_0 , $t_{\mu\nu}^{(i)}$, and $t_{\mu\nu\rho\sigma}^{(ij)}$ have been introduced in eq. (6.2) as the multipole coefficients of the spin expansion. These tensors are defined up to contributions in direction of v_i , since they drop out once contracted with the spin tensor (2.10). We can thus ensure the above relations by recasting the coefficients into the form

$$t_{\mu\nu}^{(i)} = t_{\perp,\mu\nu}^{(i)} + iq_{i,[\mu}v_{i,|\nu]}t_0, \quad (\text{B.2})$$

$$t_{\mu\nu\rho\sigma}^{(ij)} = t_{\perp,\mu\nu\rho\sigma}^{(ij)} + \frac{i}{2}t_{\perp,\mu\nu}^{(i)}q_{j,[\rho}v_{j,|\sigma]} + \frac{i}{2}q_{i,[\mu}v_{i,|\nu]}t_{\perp,\rho\sigma}^{(j)} - \quad (\text{B.3})$$

$$\frac{1}{2}q_{i,[\mu}v_{i,|\nu]}q_{j,[\rho}v_{j,|\sigma]}t_0. \quad (\text{B.4})$$

Here the index \perp means that a tensor does not contain any components in the direction v_i^μ (or v_j^μ) direction, i.e. $v_i^\mu t_{\perp,\mu\nu}^{(i)} = v_j^\rho t_{\perp,\mu\nu\rho\sigma}^{(ij)} = 0$. The expressions given in the ancillary files are not of said form but can easily be manipulated to match it without changing the waveform.

References

- [1] LIGO SCIENTIFIC, VIRGO collaboration, B. P. Abbott et al., *Observation of Gravitational Waves from a Binary Black Hole Merger*, *Phys. Rev. Lett.* **116** (2016) 061102 [[1602.03837](#)].
- [2] LIGO SCIENTIFIC, VIRGO collaboration, B. P. Abbott et al., *Binary Black Hole Mergers in the first Advanced LIGO Observing Run*, *Phys. Rev. X* **6** (2016) 041015 [[1606.04856](#)].
- [3] LIGO SCIENTIFIC, VIRGO collaboration, B. P. Abbott et al., *GW151226: Observation of Gravitational Waves from a 22-Solar-Mass Binary Black Hole Coalescence*, *Phys. Rev. Lett.* **116** (2016) 241103 [[1606.04855](#)].
- [4] LIGO SCIENTIFIC, VIRGO collaboration, B. P. Abbott et al., *GW170817: Observation of Gravitational Waves from a Binary Neutron Star Inspiral*, *Phys. Rev. Lett.* **119** (2017) 161101 [[1710.05832](#)].
- [5] LIGO SCIENTIFIC, VIRGO collaboration, B. P. Abbott et al., *GW170104: Observation of a 50-Solar-Mass Binary Black Hole Coalescence at Redshift 0.2*, *Phys. Rev. Lett.* **118** (2017) 221101 [[1706.01812](#)].
- [6] KAGRA, VIRGO, LIGO SCIENTIFIC collaboration, R. Abbott et al., *GWTC-3: Compact Binary Coalescences Observed by LIGO and Virgo during the Second Part of the Third Observing Run*, *Phys. Rev. X* **13** (2023) 041039 [[2111.03606](#)].
- [7] M. Punturo et al., *The einstein telescope: a third-generation gravitational wave observatory*, *Classical and Quantum Gravity* **27** (2010) 194002.
- [8] D. Reitze et al., *Cosmic Explorer: The U.S. Contribution to Gravitational-Wave Astronomy beyond LIGO*, *Bull. Am. Astron. Soc.* **51** (2019) 035 [[1907.04833](#)].
- [9] TIANQIN collaboration, J. Luo et al., *TianQin: a space-borne gravitational wave detector*, *Class. Quant. Grav.* **33** (2016) 035010 [[1512.02076](#)].

- [10] LISA collaboration, P. Amaro-Seoane et al., *Laser Interferometer Space Antenna*, [1702.00786](#).
- [11] M. Pürrer and C.-J. Haster, *Gravitational waveform accuracy requirements for future ground-based detectors*, *Phys. Rev. Res.* **2** (2020) 023151 [[1912.10055](#)].
- [12] S. Borhanian and B. S. Sathyaprakash, *Listening to the Universe with next generation ground-based gravitational-wave detectors*, *Phys. Rev. D* **110** (2024) 083040 [[2202.11048](#)].
- [13] R. V. Wagoner and C. M. Will, *PostNewtonian Gravitational Radiation from Orbiting Point Masses*, *Astrophys. J.* **210** (1976) 764.
- [14] C. Cutler et al., *The Last three minutes: issues in gravitational wave measurements of coalescing compact binaries*, *Phys. Rev. Lett.* **70** (1993) 2984 [[astro-ph/9208005](#)].
- [15] L. Blanchet and T. Damour, *Postnewtonian Generation of Gravitational Waves*, *Ann. Inst. H. Poincaré Phys. Theor.* **50** (1989) 377.
- [16] T. Damour and B. R. Iyer, *PostNewtonian generation of gravitational waves. 2. The Spin moments*, *Ann. Inst. H. Poincaré Phys. Theor.* **54** (1991) 115.
- [17] L. E. Kidder, C. M. Will and A. G. Wiseman, *Spin effects in the inspiral of coalescing compact binaries*, *Phys. Rev. D* **47** (1993) R4183 [[gr-qc/9211025](#)].
- [18] C. Cutler and E. E. Flanagan, *Gravitational waves from merging compact binaries: How accurately can one extract the binary's parameters from the inspiral wave form?*, *Phys. Rev. D* **49** (1994) 2658 [[gr-qc/9402014](#)].
- [19] T. A. Apostolatos, C. Cutler, G. J. Sussman and K. S. Thorne, *Spin induced orbital precession and its modulation of the gravitational wave forms from merging binaries*, *Phys. Rev. D* **49** (1994) 6274.
- [20] N. V. Krishnendu and F. Ohme, *Interplay of spin-precession and higher harmonics in the parameter estimation of binary black holes*, *Phys. Rev. D* **105** (2022) 064012 [[2110.00766](#)].
- [21] B. M. Barker and R. F. O'Connell, *Derivation of the equations of motion of a gyroscope from the quantum theory of gravitation*, *Phys. Rev. D* **2** (1970) 1428.
- [22] B. M. Barker and R. F. O'Connell, *Gravitational Two-Body Problem with Arbitrary Masses, Spins, and Quadrupole Moments*, *Phys. Rev. D* **12** (1975) 329.
- [23] L. E. Kidder, *Coalescing binary systems of compact objects to postNewtonian 5/2 order. 5. Spin effects*, *Phys. Rev. D* **52** (1995) 821 [[gr-qc/9506022](#)].
- [24] H. Tagoshi, A. Ohashi and B. J. Owen, *Gravitational field and equations of motion of spinning compact binaries to 2.5 postNewtonian order*, *Phys. Rev. D* **63** (2001) 044006 [[gr-qc/0010014](#)].
- [25] G. Faye, L. Blanchet and A. Buonanno, *Higher-order spin effects in the dynamics of compact binaries. I. Equations of motion*, *Phys. Rev. D* **74** (2006) 104033 [[gr-qc/0605139](#)].
- [26] L. Blanchet, A. Buonanno and G. Faye, *Higher-order spin effects in the dynamics of compact binaries. II. Radiation field*, *Phys. Rev. D* **74** (2006) 104034 [[gr-qc/0605140](#)].
- [27] T. Damour, P. Jaranowski and G. Schafer, *Hamiltonian of two spinning compact bodies with next-to-leading order gravitational spin-orbit coupling*, *Phys. Rev. D* **77** (2008) 064032 [[0711.1048](#)].
- [28] J. Steinhoff, S. Hergt and G. Schafer, *On the next-to-leading order gravitational spin(1)-spin(2) dynamics*, *Phys. Rev. D* **77** (2008) 081501 [[0712.1716](#)].

- [29] J. Steinhoff, G. Schafer and S. Hergt, *ADM canonical formalism for gravitating spinning objects*, *Phys. Rev. D* **77** (2008) 104018 [[0805.3136](#)].
- [30] J. Steinhoff, S. Hergt and G. Schafer, *Spin-squared Hamiltonian of next-to-leading order gravitational interaction*, *Phys. Rev. D* **78** (2008) 101503 [[0809.2200](#)].
- [31] S. Marsat, A. Bohe, G. Faye and L. Blanchet, *Next-to-next-to-leading order spin-orbit effects in the equations of motion of compact binary systems*, *Class. Quant. Grav.* **30** (2013) 055007 [[1210.4143](#)].
- [32] S. Hergt, J. Steinhoff and G. Schafer, *Reduced Hamiltonian for next-to-leading order Spin-Squared Dynamics of General Compact Binaries*, *Class. Quant. Grav.* **27** (2010) 135007 [[1002.2093](#)].
- [33] S. Hergt, J. Steinhoff and G. Schafer, *On the comparison of results regarding the post-Newtonian approximate treatment of the dynamics of extended spinning compact binaries*, *J. Phys. Conf. Ser.* **484** (2014) 012018 [[1205.4530](#)].
- [34] A. Bohe, S. Marsat, G. Faye and L. Blanchet, *Next-to-next-to-leading order spin-orbit effects in the near-zone metric and precession equations of compact binaries*, *Class. Quant. Grav.* **30** (2013) 075017 [[1212.5520](#)].
- [35] J. Hartung, J. Steinhoff and G. Schafer, *Next-to-next-to-leading order post-Newtonian linear-in-spin binary Hamiltonians*, *Annalen Phys.* **525** (2013) 359 [[1302.6723](#)].
- [36] S. Marsat, L. Blanchet, A. Bohe and G. Faye, *Gravitational waves from spinning compact object binaries: New post-Newtonian results*, 12, 2013, [1312.5375](#).
- [37] A. Bohé, G. Faye, S. Marsat and E. K. Porter, *Quadratic-in-spin effects in the orbital dynamics and gravitational-wave energy flux of compact binaries at the 3PN order*, *Class. Quant. Grav.* **32** (2015) 195010 [[1501.01529](#)].
- [38] D. Bini, A. Geralico and J. Vines, *Hyperbolic scattering of spinning particles by a Kerr black hole*, *Phys. Rev. D* **96** (2017) 084044 [[1707.09814](#)].
- [39] N. Siemonsen, J. Steinhoff and J. Vines, *Gravitational waves from spinning binary black holes at the leading post-Newtonian orders at all orders in spin*, *Phys. Rev. D* **97** (2018) 124046 [[1712.08603](#)].
- [40] R. A. Porto, *Post-Newtonian corrections to the motion of spinning bodies in NRGR*, *Phys. Rev. D* **73** (2006) 104031 [[gr-qc/0511061](#)].
- [41] R. A. Porto and I. Z. Rothstein, *The Hyperfine Einstein-Infeld-Hoffmann potential*, *Phys. Rev. Lett.* **97** (2006) 021101 [[gr-qc/0604099](#)].
- [42] R. A. Porto and I. Z. Rothstein, *Comment on ‘On the next-to-leading order gravitational spin(1) - spin(2) dynamics’ by J. Steinhoff et al*, [0712.2032](#).
- [43] R. A. Porto and I. Z. Rothstein, *Spin(1)Spin(2) Effects in the Motion of Inspiralling Compact Binaries at Third Order in the Post-Newtonian Expansion*, *Phys. Rev. D* **78** (2008) 044012 [[0802.0720](#)].
- [44] M. Levi, *Next to Leading Order gravitational Spin1-Spin2 coupling with Kaluza-Klein reduction*, *Phys. Rev. D* **82** (2010) 064029 [[0802.1508](#)].
- [45] R. A. Porto and I. Z. Rothstein, *Next to Leading Order Spin(1)Spin(1) Effects in the Motion of Inspiralling Compact Binaries*, *Phys. Rev. D* **78** (2008) 044013 [[0804.0260](#)].

- [46] R. A. Porto, *Next to leading order spin-orbit effects in the motion of inspiralling compact binaries*, *Class. Quant. Grav.* **27** (2010) 205001 [[1005.5730](#)].
- [47] M. Levi, *Next to Leading Order gravitational Spin-Orbit coupling in an Effective Field Theory approach*, *Phys. Rev. D* **82** (2010) 104004 [[1006.4139](#)].
- [48] R. A. Porto, A. Ross and I. Z. Rothstein, *Spin induced multipole moments for the gravitational wave flux from binary inspirals to third Post-Newtonian order*, *JCAP* **03** (2011) 009 [[1007.1312](#)].
- [49] J. Hartung and J. Steinhoff, *Next-to-next-to-leading order post-Newtonian spin(1)-spin(2) Hamiltonian for self-gravitating binaries*, *Annalen Phys.* **523** (2011) 919 [[1107.4294](#)].
- [50] M. Levi, *Binary dynamics from spin1-spin2 coupling at fourth post-Newtonian order*, *Phys. Rev. D* **85** (2012) 064043 [[1107.4322](#)].
- [51] R. A. Porto, A. Ross and I. Z. Rothstein, *Spin induced multipole moments for the gravitational wave amplitude from binary inspirals to 2.5 Post-Newtonian order*, *JCAP* **09** (2012) 028 [[1203.2962](#)].
- [52] M. Levi and J. Steinhoff, *Equivalence of ADM Hamiltonian and Effective Field Theory approaches at next-to-next-to-leading order spin1-spin2 coupling of binary inspirals*, *JCAP* **12** (2014) 003 [[1408.5762](#)].
- [53] M. Levi and J. Steinhoff, *Leading order finite size effects with spins for inspiralling compact binaries*, *JHEP* **06** (2015) 059 [[1410.2601](#)].
- [54] M. Levi and J. Steinhoff, *Spinning gravitating objects in the effective field theory in the post-Newtonian scheme*, *JHEP* **09** (2015) 219 [[1501.04956](#)].
- [55] M. Levi and J. Steinhoff, *Next-to-next-to-leading order gravitational spin-orbit coupling via the effective field theory for spinning objects in the post-Newtonian scheme*, *JCAP* **01** (2016) 011 [[1506.05056](#)].
- [56] M. Levi and J. Steinhoff, *Next-to-next-to-leading order gravitational spin-squared potential via the effective field theory for spinning objects in the post-Newtonian scheme*, *JCAP* **01** (2016) 008 [[1506.05794](#)].
- [57] M. Levi and J. Steinhoff, *Complete conservative dynamics for inspiralling compact binaries with spins at the fourth post-Newtonian order*, *JCAP* **09** (2021) 029 [[1607.04252](#)].
- [58] N. T. Maia, C. R. Galley, A. K. Leibovich and R. A. Porto, *Radiation reaction for spinning bodies in effective field theory I: Spin-orbit effects*, *Phys. Rev. D* **96** (2017) 084064 [[1705.07934](#)].
- [59] N. T. Maia, C. R. Galley, A. K. Leibovich and R. A. Porto, *Radiation reaction for spinning bodies in effective field theory II: Spin-spin effects*, *Phys. Rev. D* **96** (2017) 084065 [[1705.07938](#)].
- [60] M. Levi, S. Mougiakakos and M. Vieira, *Gravitational cubic-in-spin interaction at the next-to-leading post-Newtonian order*, *JHEP* **01** (2021) 036 [[1912.06276](#)].
- [61] M. Levi, A. J. Mcleod and M. Von Hippel, *N^3LO gravitational spin-orbit coupling at order G^4* , *JHEP* **07** (2021) 115 [[2003.02827](#)].
- [62] M. Levi, A. J. Mcleod and M. Von Hippel, *N^3LO gravitational quadratic-in-spin interactions at G^4* , *JHEP* **07** (2021) 116 [[2003.07890](#)].

- [63] A. Antonelli, C. Kavanagh, M. Khalil, J. Steinhoff and J. Vines, *Gravitational spin-orbit coupling through third-subleading post-Newtonian order: from first-order self-force to arbitrary mass ratios*, *Phys. Rev. Lett.* **125** (2020) 011103 [2003.11391].
- [64] M. Levi and F. Teng, *NLO gravitational quartic-in-spin interaction*, *JHEP* **01** (2021) 066 [2008.12280].
- [65] A. Antonelli, C. Kavanagh, M. Khalil, J. Steinhoff and J. Vines, *Gravitational spin-orbit and aligned $spin_1$ - $spin_2$ couplings through third-subleading post-Newtonian orders*, *Phys. Rev. D* **102** (2020) 124024 [2010.02018].
- [66] W. D. Goldberger, J. Li and I. Z. Rothstein, *Non-conservative effects on spinning black holes from world-line effective field theory*, *JHEP* **06** (2021) 053 [2012.14869].
- [67] Z. Liu, R. A. Porto and Z. Yang, *Spin Effects in the Effective Field Theory Approach to Post-Minkowskian Conservative Dynamics*, *JHEP* **06** (2021) 012 [2102.10059].
- [68] G. Cho, B. Pardo and R. A. Porto, *Gravitational radiation from inspiralling compact objects: Spin-spin effects completed at the next-to-leading post-Newtonian order*, *Phys. Rev. D* **104** (2021) 024037 [2103.14612].
- [69] J.-W. Kim, M. Levi and Z. Yin, *Quadratic-in-spin interactions at fifth post-Newtonian order probe new physics*, *Phys. Lett. B* **834** (2022) 137410 [2112.01509].
- [70] M. K. Mandal, P. Mastrolia, R. Patil and J. Steinhoff, *Gravitational spin-orbit Hamiltonian at NNNLO in the post-Newtonian framework*, *JHEP* **03** (2023) 130 [2209.00611].
- [71] M. K. Mandal, P. Mastrolia, R. Patil and J. Steinhoff, *Gravitational quadratic-in-spin Hamiltonian at NNNLO in the post-Newtonian framework*, *JHEP* **07** (2023) 128 [2210.09176].
- [72] A. Bhattacharyya, S. Ghosh and S. Pal, *Worldline effective field theory of inspiralling black hole binaries in presence of dark photon and axionic dark matter*, *JHEP* **08** (2023) 207 [2305.15473].
- [73] G. Cho, R. A. Porto and Z. Yang, *Gravitational radiation from inspiralling compact objects: Spin effects to the fourth post-Newtonian order*, *Phys. Rev. D* **106** (2022) L101501 [2201.05138].
- [74] D. Bini and T. Damour, *Gravitational spin-orbit coupling in binary systems, post-Minkowskian approximation and effective one-body theory*, *Phys. Rev. D* **96** (2017) 104038 [1709.00590].
- [75] D. Bini and T. Damour, *Gravitational spin-orbit coupling in binary systems at the second post-Minkowskian approximation*, *Phys. Rev. D* **98** (2018) 044036 [1805.10809].
- [76] J. Vines, *Scattering of two spinning black holes in post-Minkowskian gravity, to all orders in spin, and effective-one-body mappings*, *Class. Quant. Grav.* **35** (2018) 084002 [1709.06016].
- [77] J. Vines, J. Steinhoff and A. Buonanno, *Spinning-black-hole scattering and the test-black-hole limit at second post-Minkowskian order*, *Phys. Rev. D* **99** (2019) 064054 [1812.00956].
- [78] A. Guevara, *Holomorphic Classical Limit for Spin Effects in Gravitational and Electromagnetic Scattering*, *JHEP* **04** (2019) 033 [1706.02314].
- [79] A. Guevara, A. Ochirov and J. Vines, *Scattering of Spinning Black Holes from Exponentiated Soft Factors*, *JHEP* **09** (2019) 056 [1812.06895].

- [80] M.-Z. Chung, Y.-T. Huang, J.-W. Kim and S. Lee, *The simplest massive S-matrix: from minimal coupling to Black Holes*, *JHEP* **04** (2019) 156 [[1812.08752](#)].
- [81] N. Arkani-Hamed, Y.-t. Huang and D. O’Connell, *Kerr black holes as elementary particles*, *JHEP* **01** (2020) 046 [[1906.10100](#)].
- [82] A. Guevara, A. Ochirov and J. Vines, *Black-hole scattering with general spin directions from minimal-coupling amplitudes*, *Phys. Rev. D* **100** (2019) 104024 [[1906.10071](#)].
- [83] M.-Z. Chung, Y.-T. Huang and J.-W. Kim, *Classical potential for general spinning bodies*, *JHEP* **09** (2020) 074 [[1908.08463](#)].
- [84] P. H. Damgaard, K. Haddad and A. Helset, *Heavy Black Hole Effective Theory*, *JHEP* **11** (2019) 070 [[1908.10308](#)].
- [85] R. Aoude, K. Haddad and A. Helset, *On-shell heavy particle effective theories*, *JHEP* **05** (2020) 051 [[2001.09164](#)].
- [86] M.-Z. Chung, Y.-t. Huang, J.-W. Kim and S. Lee, *Complete Hamiltonian for spinning binary systems at first post-Minkowskian order*, *JHEP* **05** (2020) 105 [[2003.06600](#)].
- [87] A. Guevara, B. Maybee, A. Ochirov, D. O’connell and J. Vines, *A worldsheet for Kerr*, *JHEP* **03** (2021) 201 [[2012.11570](#)].
- [88] Z. Bern, A. Luna, R. Roiban, C.-H. Shen and M. Zeng, *Spinning black hole binary dynamics, scattering amplitudes, and effective field theory*, *Phys. Rev. D* **104** (2021) 065014 [[2005.03071](#)].
- [89] D. Kosmopoulos and A. Luna, *Quadratic-in-spin Hamiltonian at $\mathcal{O}(G^2)$ from scattering amplitudes*, *JHEP* **07** (2021) 037 [[2102.10137](#)].
- [90] W.-M. Chen, M.-Z. Chung, Y.-t. Huang and J.-W. Kim, *The 2PM Hamiltonian for binary Kerr to quartic in spin*, *JHEP* **08** (2022) 148 [[2111.13639](#)].
- [91] F. Febres Cordero, M. Kraus, G. Lin, M. S. Ruf and M. Zeng, *Conservative Binary Dynamics with a Spinning Black Hole at $\mathcal{O}(G^3)$ from Scattering Amplitudes*, *Phys. Rev. Lett.* **130** (2023) 021601 [[2205.07357](#)].
- [92] Z. Bern, D. Kosmopoulos, A. Luna, R. Roiban and F. Teng, *Binary Dynamics through the Fifth Power of Spin at $\mathcal{O}(G^2)$* , *Phys. Rev. Lett.* **130** (2023) 201402 [[2203.06202](#)].
- [93] R. Aoude, K. Haddad and A. Helset, *Searching for Kerr in the 2PM amplitude*, *JHEP* **07** (2022) 072 [[2203.06197](#)].
- [94] R. Aoude, K. Haddad and A. Helset, *Classical Gravitational Spinning-Spinless Scattering at $\mathcal{O}(G^2 S^\infty)$* , *Phys. Rev. Lett.* **129** (2022) 141102 [[2205.02809](#)].
- [95] Z. Bern, D. Kosmopoulos, A. Luna, R. Roiban, T. Scheopner, F. Teng et al., *Quantum field theory, worldline theory, and spin magnitude change in orbital evolution*, *Phys. Rev. D* **109** (2024) 045011 [[2308.14176](#)].
- [96] G. Menezes and M. Sergola, *NLO deflections for spinning particles and Kerr black holes*, *JHEP* **10** (2022) 105 [[2205.11701](#)].
- [97] M. M. Riva, F. Vernizzi and L. K. Wong, *Gravitational bremsstrahlung from spinning binaries in the post-Minkowskian expansion*, *Phys. Rev. D* **106** (2022) 044013 [[2205.15295](#)].
- [98] P. H. Damgaard, J. Hoogeveen, A. Luna and J. Vines, *Scattering angles in Kerr metrics*, *Phys. Rev. D* **106** (2022) 124030 [[2208.11028](#)].

- [99] Y. F. Bautista, A. Guevara, C. Kavanagh and J. Vines, *Scattering in black hole backgrounds and higher-spin amplitudes. Part II*, *JHEP* **05** (2023) 211 [[2212.07965](#)].
- [100] L. W. Lindwasser, *Covariant actions and propagators for all spins, masses, and dimensions*, *Phys. Rev. D* **109** (2024) 085010 [[2307.11750](#)].
- [101] J. P. Gatica, *One-Loop Observables to Higher Order in Spin*, [2412.02034](#).
- [102] A. Cristofoli, R. Gonzo, N. Moynihan, D. O’Connell, A. Ross, M. Sergola et al., *The uncertainty principle and classical amplitudes*, *JHEP* **06** (2024) 181 [[2112.07556](#)].
- [103] A. Luna, N. Moynihan, D. O’Connell and A. Ross, *Observables from the spinning eikonal*, *JHEP* **08** (2024) 045 [[2312.09960](#)].
- [104] J. P. Gatica, *The Eikonal Phase and Spinning Observables*, [2312.04680](#).
- [105] C. Heissenberg, *Angular momentum loss due to spin-orbit effects in the post-Minkowskian expansion*, *Phys. Rev. D* **108** (2023) 106003 [[2308.11470](#)].
- [106] L. W. Lindwasser, *Consistent actions for massive particles interacting with electromagnetism and gravity*, *JHEP* **08** (2024) 081 [[2309.03901](#)].
- [107] Y. F. Bautista, G. Bonelli, C. Iossa, A. Tanzini and Z. Zhou, *Black hole perturbation theory meets CFT2: Kerr-Compton amplitudes from Nekrasov-Shatashvili functions*, *Phys. Rev. D* **109** (2024) 084071 [[2312.05965](#)].
- [108] L. Cangemi, M. Chiodaroli, H. Johansson, A. Ochirov, P. Pichini and E. Skvortsov, *From higher-spin gauge interactions to Compton amplitudes for root-Kerr*, *JHEP* **09** (2024) 196 [[2311.14668](#)].
- [109] A. Brandhuber, G. R. Brown, P. Pichini, G. Travaglini and P. Vives Matasan, *Spinning binary dynamics in cubic effective field theories of gravity*, *JHEP* **08** (2024) 188 [[2405.13826](#)].
- [110] A. Brandhuber, G. R. Brown, G. Travaglini and P. Vives Matasan, *Spinning quadrupoles in effective field theories of gravity*, [2412.17958](#).
- [111] M. Alaverdian, Z. Bern, D. Kosmopoulos, A. Luna, R. Roiban, T. Scheopner et al., *Conservative Spin-Magnitude Change in Orbital Evolution in General Relativity*, *Phys. Rev. Lett.* **134** (2025) 101602 [[2407.10928](#)].
- [112] G. Chen and T. Wang, *Dynamics of spinning binary at 2PM*, *JHEP* **12** (2025) 213 [[2406.09086](#)].
- [113] D. Akpinar, F. Febres Cordero, M. Kraus, M. S. Ruf and M. Zeng, *Spinning black hole scattering at $\mathcal{O}(G^3 S^2)$: Casimir terms, radial action and hidden symmetry*, *JHEP* **03** (2025) 126 [[2407.19005](#)].
- [114] L. Bohnenblust, L. Cangemi, H. Johansson and P. Pichini, *Binary Kerr black-hole scattering at 2PM from quantum higher-spin Compton*, [2410.23271](#).
- [115] D. Bonocore, A. Kulesza and J. Pirsch, *Generalized Wilson lines and the gravitational scattering of spinning bodies*, *JHEP* **05** (2025) 034 [[2412.16049](#)].
- [116] D. Bonocore, A. Kulesza and J. Pirsch, *Higher-spin effects in black hole and neutron star binary dynamics: worldline supersymmetry beyond minimal coupling*, [2505.11488](#).
- [117] D. Akpinar, F. Febres Cordero, M. Kraus, A. Smirnov and M. Zeng, *A First Look at Quartic-in-Spin Binary Dynamics at Third Post-Minkowskian Order*, [2502.08961](#).

- [118] N. E. J. Bjerrum-Bohr, G. Chen, C. Su and T. Wang, *Kerr Black Hole Dynamics from an Extended Polyakov Action*, [2503.20538](#).
- [119] I. Vazquez-Holm and A. Luna, *Bootstrapping Classical Spinning Compton Amplitudes with Colour-Kinematics*, [2503.22597](#).
- [120] G. Mogull, J. Plefka and J. Steinhoff, *Classical black hole scattering from a worldline quantum field theory*, *JHEP* **02** (2021) 048 [[2010.02865](#)].
- [121] G. U. Jakobsen, G. Mogull, J. Plefka and B. Sauer, *All things retarded: radiation-reaction in worldline quantum field theory*, *JHEP* **10** (2022) 128 [[2207.00569](#)].
- [122] G. Kälin and R. A. Porto, *Post-Minkowskian Effective Field Theory for Conservative Binary Dynamics*, *JHEP* **11** (2020) 106 [[2006.01184](#)].
- [123] G. Kälin, J. Neef and R. A. Porto, *Radiation-reaction in the Effective Field Theory approach to Post-Minkowskian dynamics*, *JHEP* **01** (2023) 140 [[2207.00580](#)].
- [124] T. C. Quinn and R. M. Wald, *An Axiomatic approach to electromagnetic and gravitational radiation reaction of particles in curved space-time*, *Phys. Rev. D* **56** (1997) 3381 [[gr-qc/9610053](#)].
- [125] Y. Mino, M. Sasaki and T. Tanaka, *Gravitational radiation reaction to a particle motion*, *Phys. Rev. D* **55** (1997) 3457 [[gr-qc/9606018](#)].
- [126] E. Poisson, A. Pound and I. Vega, *The Motion of point particles in curved spacetime*, *Living Rev. Rel.* **14** (2011) 7 [[1102.0529](#)].
- [127] L. Barack and A. Pound, *Self-force and radiation reaction in general relativity*, *Rept. Prog. Phys.* **82** (2019) 016904 [[1805.10385](#)].
- [128] S. E. Gralla and K. Lobo, *Self-force effects in post-Minkowskian scattering*, *Class. Quant. Grav.* **39** (2022) 095001 [[2110.08681](#)].
- [129] A. Pound and B. Wardell, *Black hole perturbation theory and gravitational self-force*, [2101.04592](#).
- [130] P. Retegno, G. Pratten, L. M. Thomas, P. Schmidt and T. Damour, *Strong-field scattering of two spinning black holes: Numerical relativity versus post-Minkowskian gravity*, *Phys. Rev. D* **108** (2023) 124016 [[2307.06999](#)].
- [131] D. Kosmopoulos and M. P. Solon, *Gravitational self force from scattering amplitudes in curved space*, *JHEP* **03** (2024) 125 [[2308.15304](#)].
- [132] C. Cheung, J. Parra-Martinez, I. Z. Rothstein, N. Shah and J. Wilson-Gerow, *Effective Field Theory for Extreme Mass Ratio Binaries*, *Phys. Rev. Lett.* **132** (2024) 091402 [[2308.14832](#)].
- [133] C. Cheung, J. Parra-Martinez, I. Z. Rothstein, N. Shah and J. Wilson-Gerow, *Gravitational scattering and beyond from extreme mass ratio effective field theory*, *JHEP* **10** (2024) 005 [[2406.14770](#)].
- [134] M. Driesse, G. U. Jakobsen, G. Mogull, J. Plefka, B. Sauer and J. Usovitsch, *Conservative Black Hole Scattering at Fifth Post-Minkowskian and First Self-Force Order*, *Phys. Rev. Lett.* **132** (2024) 241402 [[2403.07781](#)].
- [135] M. Driesse, G. U. Jakobsen, A. Klemm, G. Mogull, C. Nega, J. Plefka et al., *Emergence of Calabi-Yau manifolds in high-precision black-hole scattering*, *Nature* **641** (2025) 603 [[2411.11846](#)].

- [136] D. Akpinar, V. del Duca and R. Gonzo, *The spinning self-force EFT: 1SF waveform recursion relation and Compton scattering*, [2504.02025](#).
- [137] P. D. D’Eath, *High Speed Black Hole Encounters and Gravitational Radiation*, *Phys. Rev. D* **18** (1978) 990.
- [138] S. J. Kovacs and K. S. Thorne, *The Generation of Gravitational Waves. 3. Derivation of Bremsstrahlung Formulas*, *Astrophys. J.* **217** (1977) 252.
- [139] S. J. Kovacs and K. S. Thorne, *The Generation of Gravitational Waves. 4. Bremsstrahlung*, *Astrophys. J.* **224** (1978) 62.
- [140] G. U. Jakobsen, G. Mogull, J. Plefka and J. Steinhoff, *Classical Gravitational Bremsstrahlung from a Worldline Quantum Field Theory*, *Phys. Rev. Lett.* **126** (2021) 201103 [[2101.12688](#)].
- [141] S. Mougiakakos, M. M. Riva and F. Vernizzi, *Gravitational Bremsstrahlung in the post-Minkowskian effective field theory*, *Phys. Rev. D* **104** (2021) 024041 [[2102.08339](#)].
- [142] G. U. Jakobsen, G. Mogull, J. Plefka and J. Steinhoff, *Gravitational Bremsstrahlung and Hidden Supersymmetry of Spinning Bodies*, *Phys. Rev. Lett.* **128** (2022) 011101 [[2106.10256](#)].
- [143] S. De Angelis, P. P. Novichkov and R. Gonzo, *Spinning waveforms from the Kosower-Maybee-O’Connell formalism at leading order*, *Phys. Rev. D* **110** (2024) L041502 [[2309.17429](#)].
- [144] R. Aoude, K. Haddad, C. Heissenberg and A. Helset, *Leading-order gravitational radiation to all spin orders*, *Phys. Rev. D* **109** (2024) 036007 [[2310.05832](#)].
- [145] A. Brandhuber, G. R. Brown, G. Chen, J. Gowdy and G. Travaglini, *Resummed spinning waveforms from five-point amplitudes*, *JHEP* **02** (2024) 026 [[2310.04405](#)].
- [146] A. Herderschee, R. Roiban and F. Teng, *The sub-leading scattering waveform from amplitudes*, *JHEP* **06** (2023) 004 [[2303.06112](#)].
- [147] A. Brandhuber, G. R. Brown, G. Chen, S. De Angelis, J. Gowdy and G. Travaglini, *One-loop gravitational bremsstrahlung and waveforms from a heavy-mass effective field theory*, *JHEP* **06** (2023) 048 [[2303.06111](#)].
- [148] A. Georgoudis, C. Heissenberg and I. Vazquez-Holm, *Inelastic exponentiation and classical gravitational scattering at one loop*, *JHEP* **06** (2023) 126 [[2303.07006](#)].
- [149] A. Elkhidir, D. O’Connell, M. Sergola and I. A. Vazquez-Holm, *Radiation and reaction at one loop*, *JHEP* **07** (2024) 272 [[2303.06211](#)].
- [150] L. Bohnenblust, H. Ita, M. Kraus and J. Schlenk, *Gravitational Bremsstrahlung in black-hole scattering at $\mathcal{O}(G^3)$: linear-in-spin effects*, *JHEP* **11** (2024) 109 [[2312.14859](#)].
- [151] D. A. Kosower, B. Maybee and D. O’Connell, *Amplitudes, Observables, and Classical Scattering*, *JHEP* **02** (2019) 137 [[1811.10950](#)].
- [152] B. Maybee, D. O’Connell and J. Vines, *Observables and amplitudes for spinning particles and black holes*, *JHEP* **12** (2019) 156 [[1906.09260](#)].
- [153] A. Cristofoli, R. Gonzo, D. A. Kosower and D. O’Connell, *Waveforms from amplitudes*, *Phys. Rev. D* **106** (2022) 056007 [[2107.10193](#)].

- [154] D. Bini, T. Damour, S. De Angelis, A. Geralico, A. Herderschee, R. Roiban et al., *Gravitational waveforms: A tale of two formalisms*, *Phys. Rev. D* **109** (2024) 125008 [[2402.06604](#)].
- [155] C.-H. Shen, *Gravitational Radiation from Color-Kinematics Duality*, *JHEP* **11** (2018) 162 [[1806.07388](#)].
- [156] S. Abreu, J. Dormans, F. Febres Cordero, H. Ita, M. Kraus, B. Page et al., *Caravel: A C++ framework for the computation of multi-loop amplitudes with numerical unitarity*, *Comput. Phys. Commun.* **267** (2021) 108069 [[2009.11957](#)].
- [157] S. Caron-Huot, M. Giroux, H. S. Hannesdottir and S. Mizera, *What can be measured asymptotically?*, *JHEP* **01** (2024) 139 [[2308.02125](#)].
- [158] G. U. Jakobsen and G. Mogull, *Linear response, Hamiltonian, and radiative spinning two-body dynamics*, *Phys. Rev. D* **107** (2023) 044033 [[2210.06451](#)].
- [159] Y. F. Bautista, *Dynamics for super-extremal Kerr binary systems at $O(G^2)$* , *Phys. Rev. D* **108** (2023) 084036 [[2304.04287](#)].
- [160] G. U. Jakobsen, G. Mogull, J. Plefka and J. Steinhoff, *SUSY in the sky with gravitons*, *JHEP* **01** (2022) 027 [[2109.04465](#)].
- [161] K. Haddad, G. U. Jakobsen, G. Mogull and J. Plefka, *Spinning bodies in general relativity from bosonic worldline oscillators*, *JHEP* **02** (2025) 019 [[2411.08176](#)].
- [162] A. Brandhuber, G. R. Brown, G. Chen, G. Travaglini and P. Vives Matasan, *Spinning waveforms in cubic effective field theories of gravity*, *JHEP* **12** (2024) 039 [[2408.00587](#)].
- [163] J. S. Schwinger, *Brownian motion of a quantum oscillator*, *J. Math. Phys.* **2** (1961) 407.
- [164] L. V. Keldysh, *Diagram technique for nonequilibrium processes*, *Zh. Eksp. Teor. Fiz.* **47** (1964) 1515.
- [165] C. Cheung, N. Shah and M. P. Solon, *Mining the Geodesic Equation for Scattering Data*, *Phys. Rev. D* **103** (2021) 024030 [[2010.08568](#)].
- [166] A. Brandhuber, G. Chen, G. Travaglini and C. Wen, *Classical gravitational scattering from a gauge-invariant double copy*, *JHEP* **10** (2021) 118 [[2108.04216](#)].
- [167] S. S. Chava, *Classical gravitational scattering from amplitudes and geometry*, Master’s thesis, Swiss Federal Institute of Technology, 2023.
- [168] G. Brunello and S. De Angelis, *An improved framework for computing waveforms*, *JHEP* **07** (2024) 062 [[2403.08009](#)].
- [169] F. V. Tkachov, *A theorem on analytical calculability of 4-loop renormalization group functions*, *Phys. Lett. B* **100** (1981) 65.
- [170] K. G. Chetyrkin and F. V. Tkachov, *Integration by parts: The algorithm to calculate β -functions in 4 loops*, *Nucl. Phys. B* **192** (1981) 159.
- [171] S. Laporta, *High-precision calculation of multiloop Feynman integrals by difference equations*, *Int. J. Mod. Phys. A* **15** (2000) 5087 [[hep-ph/0102033](#)].
- [172] P. Nogueira, *Automatic Feynman Graph Generation*, *J. Comput. Phys.* **105** (1993) 279.
- [173] J. M. M.-G. et al., “xact: Efficient tensor computer algebra.” <http://www.xact.es/>, 2025.
- [174] T. Nutma, *xTras : A field-theory inspired xAct package for mathematica*, *Comput. Phys. Commun.* **185** (2014) 1719 [[1308.3493](#)].

- [175] V. Magerya, “alibrary.” <https://github.com/magv/alibrary>, 2025.
- [176] R. N. Lee, *Presenting LiteRed: a tool for the Loop InTEgrals REDuction*, [1212.2685](#).
- [177] R. N. Lee, *LiteRed 1.4: a powerful tool for reduction of multiloop integrals*, *J. Phys. Conf. Ser.* **523** (2014) 012059 [[1310.1145](#)].
- [178] P. H. Damgaard, E. R. Hansen, L. Planté and P. Vanhove, *The relation between KMOC and worldline formalisms for classical gravity*, *JHEP* **09** (2023) 059 [[2306.11454](#)].
- [179] V. Vaidya, *Gravitational spin Hamiltonians from the S matrix*, *Phys. Rev. D* **91** (2015) 024017 [[1410.5348](#)].
- [180] R. U. Sexl and H. K. Urbantke, *Relativity Groups, Particles. : Special Theory of Relativity as the Basis of Field and Elementary Particle Physics*. Springer, Wien, 1976, [10.1007/978-3-7091-6234-7](#).
- [181] L. Cangemi and P. Pichini, *Classical limit of higher-spin string amplitudes*, *JHEP* **06** (2023) 167 [[2207.03947](#)].
- [182] S. Weinberg, *Infrared photons and gravitons*, *Phys. Rev.* **140** (1965) B516.
- [183] W. D. Goldberger and A. Ross, *Gravitational radiative corrections from effective field theory*, *Phys. Rev. D* **81** (2010) 124015 [[0912.4254](#)].
- [184] I. I. Shapiro, *Fourth Test of General Relativity*, *Phys. Rev. Lett.* **13** (1964) 789.
- [185] H. Bondi, M. G. J. van der Burg and A. W. K. Metzner, *Gravitational waves in general relativity. 7. Waves from axisymmetric isolated systems*, *Proc. Roy. Soc. Lond. A* **269** (1962) 21.
- [186] R. K. Sachs, *Gravitational waves in general relativity. 8. Waves in asymptotically flat space-times*, *Proc. Roy. Soc. Lond. A* **270** (1962) 103.
- [187] G. Veneziano and G. A. Vilkovisky, *Angular momentum loss in gravitational scattering, radiation reaction, and the Bondi gauge ambiguity*, *Phys. Lett. B* **834** (2022) 137419 [[2201.11607](#)].
- [188] A. Georgoudis, C. Heissenberg and R. Russo, *An eikonal-inspired approach to the gravitational scattering waveform*, [2312.07452](#).
- [189] A. Georgoudis, C. Heissenberg and R. Russo, *Post-Newtonian multipoles from the next-to-leading post-Minkowskian gravitational waveform*, *Phys. Rev. D* **109** (2024) 106020 [[2402.06361](#)].
- [190] A. Elkhidir, D. O’Connell and R. Roiban, *Supertranslations from Scattering Amplitudes*, [2408.15961](#).
- [191] X. Liu and Y.-Q. Ma, *AMFlow: A Mathematica package for Feynman integrals computation via auxiliary mass flow*, *Comput. Phys. Commun.* **283** (2023) 108565 [[2201.11669](#)].
- [192] A. Georgoudis, C. Heissenberg and I. Vazquez-Holm, *Addendum to: Inelastic exponentiation and classical gravitational scattering at one loop*, *JHEP* **2024** (2024) 161 [[2312.14710](#)].
- [193] T. Adamo and R. Gonzo, *Bethe-Salpeter equation for classical gravitational bound states*, *JHEP* **05** (2023) 088 [[2212.13269](#)].
- [194] T. Adamo, R. Gonzo and A. Ilderton, *Gravitational bound waveforms from amplitudes*, *JHEP* **05** (2024) 034 [[2402.00124](#)].
- [195] C. Heissenberg, *Radiation-Reaction and Angular Momentum Loss at $\mathcal{O}(G^4)$* , [2501.02904](#).

[196] B. Latosh, *FeynGrav 2.0*, *Comput. Phys. Commun.* **292** (2023) 108871 [[2302.14310](#)].